Aalto University
School of Chemical
Engineering

Yuhang Ye

COATING REGENERATED CELLULOSE FIBERS WITH GOLD NANOPARTICLES FOR UV-PROTECTION AND ANTI-BACTERIAL PROPERTIES

Master´s Programme in Chemical, Biochemical and Materials Engineering
Major in Chemistry

Master's thesis for the degree of Master of Science in Technology submitted for inspection, Espoo, 07 July, 2018.

Supervisor	Professor Sixta Herbert
Instructor	M. Sc. Simone Haslinger

Aalto University
School of Chemical
Engineering

Aalto University, P.O. BOX 11000, 00076 AALTO
www.aalto.fi

Abstract of master's thesis

Author Yuhang Ye

Title of thesis Coating regenerated cellulose fibers with gold nanoparticles for UV-protection and anti-bacterial properties

Degree Programme Master´s Programme in Chemical, Biochemical and Materials Engineering

Major Chemistry

Thesis supervisor Professor Sixta Herbert

Thesis advisor(s) / Thesis examiner(s) M. Sc. Simone Haslinger

Date 04.07.2018 **Number of pages** 66 **Language** English

Abstract

A facile green synthesis route for gold nanoparticles (AuNPs) was developed to realize multifunction for Ioncell fabrics. Bleached birch pulp was used to prepare gold nanoparticles (AuNPs) by reducing chloroauric acid (CA) in situ on cellulose, forming cellulose-AuNPs compounds. The color of pulp changed from white to purple due to the localized surface plasmon resonance (LSPR) effect of AuNPs. Subsequently, the obtained colored pulp was utilized to spin fibers after dissolving in the [DBNH][OAc]. And finally, the fabrics were knitted for the end-use.

During this process, factors including the added amount of CA solution, pH, the addition of CTAB, and the combination of silver ions, were studied. The Ioncell fibers treated with AuNPs showed good mechanical properties. Moreover, the AuNPs endowed Ioncell fabrics with excellent washing fastness and strong UV protection property.

Keywords Gold nanoparticles, Ioncell fibers, coloration, in-situ synthesis, UV blocking

Foreword

Time flies, I have been in the spinning group for six months starting from the last summer. I would like to express my gratitude to all of those who helped me during the writing of this thesis.

At first, my deepest gratitude goes to Professor Sixta Herbert, my supervisor, for offering this great opportunity and interesting topic to me.

Secondly, I would like to give my heartfelt gratitude to my advisor Simone Haslinger, for her constant encouragement and guidance over these six months. She supported me throughout all the stages of this master thesis, from lab work to writing. Without her contribution and illuminating instruction, this thesis would have not had the possibility to reach its present form.

I am also greatly indebted to my colleagues in the spinning research group: Xueyao Ge, Kaniz Moriam, and Marja Rissanen, who helped me a lot in the past six months.

Lastly, my thanks go to my beloved family, for their loving considerations and great confidence in me, all through these years, and to my lovely friends who gave me help and time in supporting me when I met problems, during these two years of my master studies.

11th June 11, 2018
Yuhang Ye

Contents

Abbreviations

Gold nanoparticles	AuNPs
1,5-diazabicyclo[4.3.0]non-5-ene acetate	[DBNH] OAc
Degree of polymerization	DP
Ionic liquids	ILs
1-ethyl-3-methylimidazolium acetate	[EMIM] OAc
1-butyl-3-methylimidazolium acetate	[BMIM] OAc
Surface plasmon resonance	SPR
Localized surface plasmon resonance	LSPR
Metal nanoparticles	MNPs
Nanorods	NRs
Longitudinal plasmon band	LPB
Transverse plasmon band	TPB
Surface plasmon band	SPB
Trichloride cellulose	TC
Methyl cellulose	MC
1,4-diaminobutane	DAB
Poly (diallyldimethylammonium chloride)	PDDA
Nanocrystalline	NCC
1,6-di-aminohexane	DAH
Tris(2-aminoethyl) amine	TAEA
(2,2,6,6-tetramethylpiperidin-1-yl)oxidanyl	TEMPO
Thiosemicarbazide	TSC
Surface enhanced raman scattering	SERS
Epichlorohydrine	ECH
N-aminoguanidine	NA
Ultraviolet	UV
UV protection factor	UPF
Silver nanoparticles	AgNPs
Chloroauric acid	CA
Hydrochloric acid	HCl
Sodium hydroxide	NaOH
Dry matter content	DMC
Hexadecyltrimethylammonium bromide	CTAB
Oven dried	OD
Gel permeation chromatography	GPC
Transmission electron microscopy	TEM
Scanning electron microscope	SEM

1. Introduction

Gold nanoparticles (AuNPs) have gained much attention in recent years because of their diverse chemical, physical, optical, magnetic properties.[1,2] Compared to bulky golden molecules, gold nanoparticles have more excellent properties in aspects of optics due to a phenomenon called surface plasmon resonance.[3] This phenomenon can lead to strong light absorption and scattering, thereby offering various interesting applications including surface-enhanced Raman scattering, and biological sensing.[4]

Besides, surface plasmon resonance can enhance the Mole extinction coefficient because of the large scattering and absorbing the cross section of gold nanoparticles.[5] Therefore, gold nanoparticles are able to display vivid colors by tuning their aspect ratio.[6] This phenomenon had been discovered and applied by our ancestors. A wide range of metal nanoparticles have been utilized as pigments for coloring window glass and for dyeing ceramics.[7] Recently, gold nanoparticles as pigments for dyeing textile materials re-emerge into our research fields, because they not only bring about gorgeous colors, but also extend the functionality of textiles to enable anti-bacterial properties, UV protection, and catalysis.[8–10]

Traditionally, gold nanoparticles are prepared at first by the addition of reduction chemicals to reduce a gold precursor such as chloroauric acid into gold nanoparticles in an aqueous solution. Gold nanoparticles easily aggregate into large particles, which reduces their different advantages by reducing the specific surface area. Therefore, stabilizers have to be added into the solution of gold nanoparticles. Subsequently, a textile is dipped into the resulting solution and gold nanoparticles are coated on the surface of the textiles because of electrostatic effects.[8]

It is evident that this conventional approach is complicated and time-consuming. Furthermore, reduction and stabilization chemicals could be transferred to the textile and cause toxic effects. In addition, as stated previously, the gold nanoparticles are coated onto the textile through electrostatic effects, which are relatively weak bonding forces, so that the attached gold nanoparticles might not be stable enough to fulfill a

commercial use.[11]

Therefore, exploring an ecological and sustainable pathway for combing AuNPs with textiles has gained much interests recently. Cellulose as a sustainable polymer has the ability to be an alternative fiber material for embedding AuNPs. So far, several studies have been conducted to contribute in this direction. It has been reported that Gold nanoparticles have been successfully synthesized from pulp[8], wood[12] or, Ramie[9] using a one-pot reaction. Thereby, cellulose plays the role of a mini-reactor, hydroxyl and hemiacetal groups serve as reducing agents and stabilizers, respectively, instead of chemicals.

However, these studies still have some limitations. First of all, they used unbleached wood pulp or wool as raw materials. It implies that the raw materials have their own color, which by interference with the original colors can create obstacles in matching the final color of a fabric. In addition, none of these studies continued to use the coated pulp for dry-jet wet spinning to produce cellulose fibers and to make real fabrics by yarn spinning and knitting, which has not been introduced to industry yet.

In this study, we utilized bleached birch pulp (Enocell pulp) as substrate for in-situ synthesis of gold nanoparticles using $HAuCl_4$ as precursor without any other further chemicals. Then the coated pulp was dissolved in [DBNH] OAc to prepare a dope to spin colored staple fibers by dry-jet wet spinning successfully. The staple fibers were processed into yarn and further knitted into real fabrics. The mechanical properties of the staple fibers and yarns were measured and their wash fastness, UV-protection, and anti-bacterial properties were evaluated.

2. Literature review

2.1 Cellulose

2.1.1 Structure of cellulose

Cellulose, as the most abundant biopolymers on earth, was discovered in 1838 and has been employed to produce polymer materials since 1870.[12] Apart from plants, which are the main source for cellulose, it can be obtained from cell walls of several marine animals, algae, fungi, and bacteria.[13]

As shown in Figure 1, cellulose is a linear polymer, which is composed of two anhydroglucose sugar units, which are covalently connected through an oxygen bonded to the C_1 of one glucose ring and the C_4 of the adjoining ring (1 - 4 linkage). The formed bonds are so called β1–4 glucosidic bonds. The length of a cellulose chain depends on the number of repeating units of glucose, which is defined as the degree of polymerization (DP). [13] Cellulose from various sources have different DPs, ranging from 20 in the case of synthesized cellulose, and to 10000 or more for bacterial cellulose. Wood-based cellulose contains 10000 repeating units in general, and one side of each chain has a hemiacetal group at the C_1 position and one alcoholic hydroxyl group on the C_4 on the other side. They are commonly called reducing group and non-reducing group, respectively..[14] Consequently, the mechanical properties of plant fibers depend on the cellulose content, DP and the lateral arrangement of the microfibrils.[15]

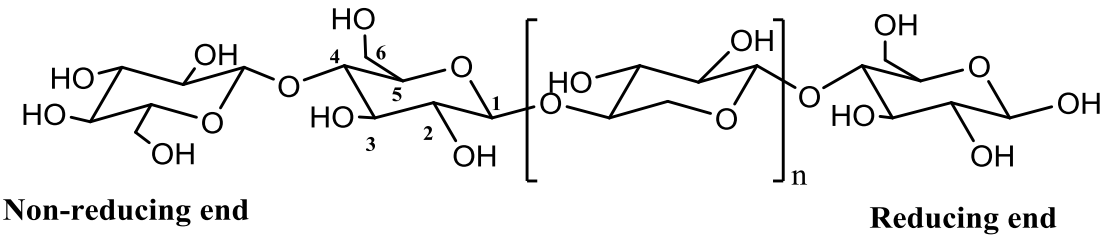

Figure 1. The polymer chains of cellulose

Apart from the β1-4 glucosidic bond, cellulose is stabilized by a large amount of inter and intra hydrogen bonds between the C_3 hydroxyl group and the adjacent in-ring oxygen, as well as between the C_2 hydroxyl group and the hydroxy methyl oxygen on the C_6, resulting in the formation of a specific microfibril structure.

This structure is composed of two regions. One is a highly structured crystalline part due to the hydrogen bonds between the C_6 hydroxy methyl and the C_3 hydroxy groups of the adjacent chains. The other one is an amorphous domain, which is defined as the region of the fiber where there is no longer the order of chain molecules. Beside these two areas, microfibrils exit in the secondary cell wall, crosslinking hemicellulose to lignin, which will be isolated prior to cellulose are applied.[16–18]

Native cellulose (Cellulose I), as the most crystalline type, is composed of two different categories: I_α and I_β, which have triclinic and monoclinic unit cells respectively. These are present in natural cellulose, but the content varies according to the sources of cellulose. Cellulose I can be converted into Cellulose II by mercerization or regeneration. In addition to Cellulose I, II, , a variety of other structures of cellulose have been explored, such as cellulose III and cellulose IV.[13,19]

The mechanical properties of cellulose depend on the molecular structure of the different allomorphs. During the general deformation process on cellulose, complicated and greatly different stretching and re-organization mechanisms occur on the hydrogen bonds in the amorphous and crystalline regions, resulting in varied tensile properties. Amorphous cellulose was calculated to show an average Young's modulus of 10.3 GPa, while the corresponding value of ramie fibers achieves up to 134 Gpa.[20] Cellulose I was found to have a modulus of 138 GPa, whereas cellulose IV exhibited a lower value of 75 GPa.[21] Compared to engineering materials such as aluminums (70 GPa) or glass fibers (76 GPa), the mechanical properties of cellulose perform well.[22] Due to its excellent tensile properties and low density, cellulose has been recognized as one of the most potential candidates in the polymer family.

2.1.2 Solubility of cellulose

Because of numerous inter and intra hydrogen bonds, cellulose is not melting and is insoluble in most solvents. Besides, its crystalline properties prevent cellulose from being hydrolyzed by acid and base, thereby making a chemical processing of cellulose difficult.[23] Hence, finding a proper solvent to dissolve cellulose for the successful utilization of cellulose as a component of polymeric materials has been a serious issue to be solved in the cellulose field.

So far, a widely used approach is the viscose process which was invented over 100 years ago.[24] In this procedure, CS_2 reacts with alkali cellulose (sodium cellulosate) to cellulose xanthogenate by derivatization. Then, the resulting molecules dissolve in aqueous NaOH to form a viscose solution. Subsequently, the cellulose derivative is regenerated in an aqueous sulfuric acid and sodium sulfate solution. During the regeneration of viscose to fibers, CS_2 and hydrogen sulfide is generated which causes environmental problems due to its toxicity, flammability and explosiveness. Producers have developed many techniques to improve the viscose process and to reduce its negative effect on environment. For instance, they made an effort to decrease the emission of toxic gases and recycle CS_2, while the generation of waste water is still problematic.

Because of this situation, it is crucial to develop a process to dissolve regenerated cellulose fibers with high sustainability, eco-friendliness and low costs. N-methyl-morpholine N-oxide monohydrate (NMMO.H_2O) was currently the only direct cellulose solvent that led to commercial application in the production of regenerated cellulose fibers using a dry-jet wet spinning process.[25] Despite its excellent dissolution and spinning properties, NMMO has some intrinsic shortcomings such as its chemical and thermal instability which affords the addition of stabilizers. Further, the high viscosity of the cellulose solution in NMMO monohydrate already at moderate polymer concentrations of e.g. 13 wt% sets limits in the process economy.[26] Certain ionic liquids

(ILs) with a high hydrogen bond basicity and not too high hydrogen acidity have shown to be excellent cellulose solvents as reported by Rogers and his coworkers in 2002. They proved that ILs are quite good for both, cellulose dissolution and regeneration, opening new world to the cellulose research community.[27]

Ionic liquids are referred to as a group of salts, which are liquid at relatively low temperatures (less than 100◦C), usually composed of anions and cations. Compared to other types of solvents, ILs have a number of attractive features, including non-flammability, chemical and physical stability and environmental friendliness.[28] Until now, a variety of IL systems have been exploited including [EMIM] OAc, [BMIM] OAc, and [DBNH]OAc as cellulose solvents.[29–31]

In order to control the cellulose dissolution procedure, the mechanism behind has been investigated over a long term. These studies demonstrate that both, anions and cations, have equally important roles in the dissolution. The anions connect to hydroxyls of cellulose and the cations react with polysaccharides through hydrophobic interactions. At first, the basic anions interact with the hydroxyl groups on cellulose to break down the hydrogen bond network in the cellulose matrix while the hydrophobic groups of cellulose interact with the imidazolium ring of ILs through hydrophobic interactions. In addition, the acidic proton at the C_2 position of the imidazolium of ILs ring interacts with the cellulose' hydroxyl groups.

2.2 Gold nanoparticles

2.2.1 Surface plasmon resonance

In recent decades, gold nanoparticles (AuNPs) have extensively been researched in the field of nanotechnology and nanoscience due to their distinct properties, in optoelectronics, and catalysis, their excellent biocompatibility, and low toxicity.[32–34] Among these properties, surface plasmon resonance (SPR) has gained the most attention. Like electromagnetic radiation has photons and mechanical vibration has

phonons, plasma oscillation has plasmons. A plasmon is a quasi-particle defined as a quantum of plasma oscillation, commonly observed in metals. Metallic bonding consists of a negative electron cloud surrounding positive nuclei. This negative electron cloud oscillates around their equilibrium positions around the positive nuclei. SPR occurs when resonant oscillation of conduction electrons is stimulated by incident light at the interface of negative and positive permittivity materials.[35]

However, SPR can only occur in bulky gold (e.g. film, coating). Once the size of gold nanoparticles reaches a range of 1 nm – 100 nm, or even smaller than the wavelength of the incident light, surface plasmon resonance is more accurately described as localized surface plasmon resonance (LSPR).[36] The mechanisms of LSPR is similar to SPR: When incident light interacts with AuNPs, the electromagnetic field of the light induces a collective coherent oscillation of the surface electrons on the metal nanoparticles (MNPs) in resonance with the frequency of light. A charge separation between the free electrons and the ionic metal core will be electronically initiated due to the interaction between the free electrons of the nanoparticles and the electric field of the light. Among the free electrons, the Coulomb repulsion is caused to move the free electrons acting as a restoring force, in the opposite direction, which results in the collective oscillation of electrons.[36,37]

In addition, the occurrence of LSPR can induce a strong absorption of light. Compared to SPR, LSPR possesses more interesting optical properties. A significant example is the color of gold. The color of gold nanoparticles is unlike the traditional 'gold color', as it can rather display a series of colors (e.g. purple, pink, and red).[38]

LSPR essentially depends on two factors, such as the materials used and the size and shape of the gold nanoparticles. Through adjusting these parameters, the LSPR wavelength will be tuned within the overall visible region and thus displaying a variety of characteristic colors.[34,39]

2.2.1 Spherical gold nanoparticles and gold nanorods

In general, AuNPs can be categorized as spherical Au NPs and nanorods (NRs)

based on their morphology. Spherical Au nanoparticles in solution show a range of colors including purple, orange, and pink due to the different size of the core nanoparticles (1-100 nm), and generally show a size dependent absorption peak from 500 to 550 nm in the spectrum (Figure 2).[40] This peak is named 'surface plasmon band'(SPB), which is caused by the excitation of LSPR.[41]

Since gold NRs have two types of electron oscillations along the long and the short axes, two surface plasmon bands can be observed in their absorbance spectrum, as illustrated in the Figure 3.[39] The one along the long axis is called the longitudinal plasmon band (LPB) and the other one along the short axis is defined as the transverse plasmon band (TPB). The TPB of AuNRs shows a peak around 550nm and is not sensitive to changes of size. On the contrary, the position of the peak of the LPB can be tuned in a wide range from 300 nm to 1100 nm by manipulating the aspect ratio of the nanoparticles, which is also a reason why nanorods can display more colors than spherical Au particles.[3] Furthermore, with the increase of the aspect ratio of nanorods, the LPB shows a red-shift.[41]

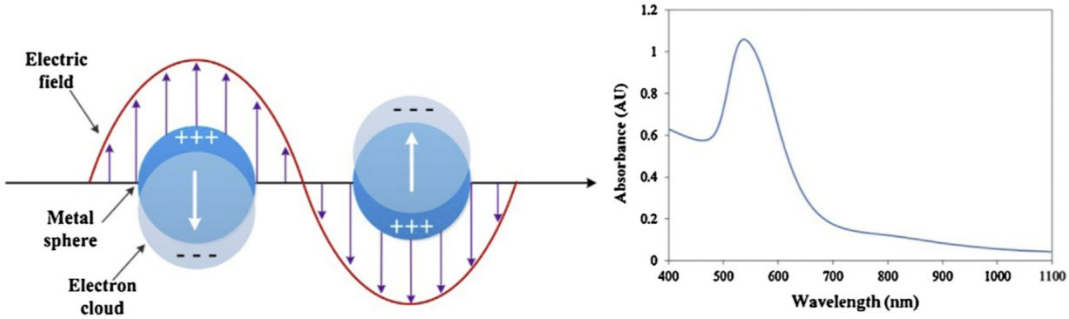

Figure 2. Schematic illustration of LSPR excitation for spherical AuNPs and a typical absorption band for spherical AuNPs[42](Copy from Ref.42)

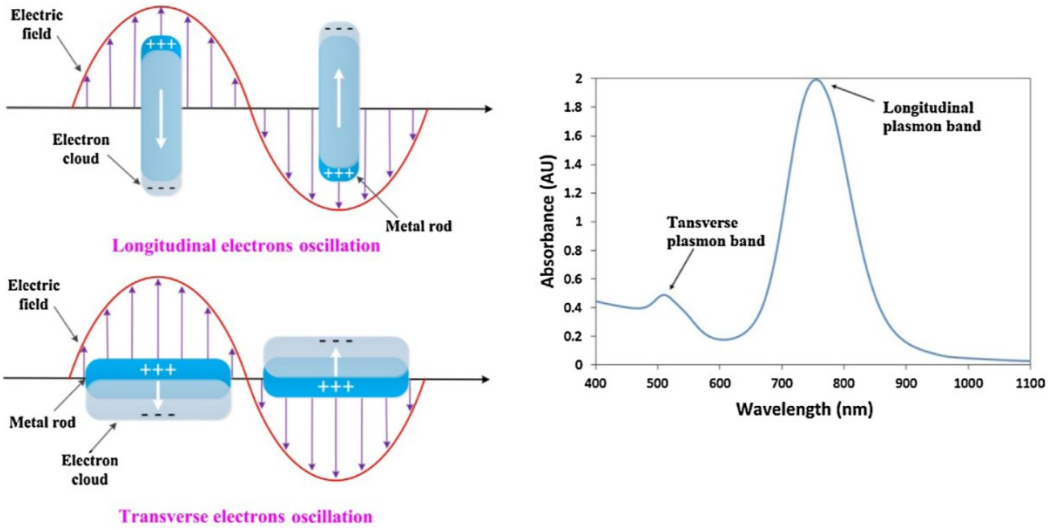

Figure 3. Schematic illustration of LSPR excitation for AuNRs and two typical absorption bands for AuNRs[42](Copy from Ref.42)

In addition, solvent, surface ligands, core charge, and temperature also have significant effects on the wavelength of the surface plasmon band as they influence the electron charge density on the surface of the particles.[33,43] Interestingly, Hu et al. also found that the aggregation of nanoparticles was another factor that affected the charge density. They reported that as a result of the inter-particle plasmon coupling, the LSPR frequency showed a significant red shift, resulting in the broadening of the surface plasmon band thereby changing the color of the nanorod solution from red to blue. [44]

As demonstrated in the *Figure 2 and 3*, the LSPR is capable of causing a strong light absorption. In the case of spherical AuNPs, this phenomenon can be explained by the Maxwell equation. Based on the Mie theory, the extinction cross-section of nanoparticles with a certain radius R and sufficient purity, can be illustrated by the equation below. [45,46]

$$c_{ext} \equiv \frac{24\pi^2 R^3 N \varepsilon_m^{3/2}}{\lambda} \frac{\varepsilon_i}{(\varepsilon_r + 2\varepsilon_m)^2 + \varepsilon_i^2}$$

Where ε_m is the dielectric constant of the surrounding medium, ε_r and ε_i are the real and imaginary part of the dielectric function of the MNPs, respectively, and N is the number of spheres per unit volume.

When $\varepsilon_r = -2\varepsilon_m$, then SPB will appear. Calculated according to the above equation,

the SPB of gold is in the visible light range, which explains why the color of nanoparticles caused by PLSR can be recognized by human eye.

Zhong *et.al.* used the Mie theory and equation to successfully simulate the LSPR band, which is similar to bands caused by spherical AuNPs.[47] They found that spherical AuNPs of each size could form a LSPR band around a wavelength of 550 nm in the spectrum and that these bands displayed an obvious red shift with an increasing size of the AuNPs. A comparison between the absorption bands as well as the wavelengths from simulated spectra and the real experimental results was performed, showing excellent agreement.

Contrary to spherical AuNPs, Gans found that AuNRs can be described by a dipole approximation. As a result of surface curvature and their geometry, AuNRs produce two types of surface plasmon modes in both transverse and longitudinal direction. Therefore, they are treated as ellipsoids when explaining the optical properties of gold nanorods. According to Gans' theory, the area of the extinction cross-section is represented by an equation more complex than the Mie theory. Consequently, any small change in the aspect ratio of the nanorods results in a significant change in the plasmon band.[48,49]

Similarly, the relationship between simulated plasmon resonance spectra and the aspect ratio of AuNRs was studied by EI-Sayed et al. using Gan's theory. In their study, two LSPR bands named TPB and LPB, respectively, could also be observed in the same spectrum as demonstrated in Figure 3. With an increasing aspect ratio of the AuNRs, TPB shows a small blue shift while the LPB exhibits a large red shift. Moreover, a positive correlation was found between the peak wavelength of the LPB and the aspect ratio confirming empirical results. Besides, the LPB was found to be more sensitive to the change of the surrounding environment in comparison to TPB. When the dielectric constant of the surrounding medium was increased, the wavelengths originating from TPB and LPB changed. Both TPB and LPB showed a red shift, with the one of LPB being however much more significant.[50]

2.3 Methods utilized for the preparation of cellulose-AuNPs composite materials

Cellulose, as a renewable organic biomaterial with high abundance, has been a strong candidate in the pool of templates for the preparation of AuNPs-hybrids due to their unique properties. For instance, polymers and carbon materials cannot be considered for biomedical use because they lack good biocompatibility which results in the inactivation of biological enzymes.[51] Although hard materials like nanotubes have been reported in the preparation of hybrids in combination with AuNPs, they also have some limitations including not being biodegradable, and toxic to organisms.[52] However, cellulose can be used as an idealized solution for these problems of traditional materials due to its proven biocompatibility, biodegradability and non-toxicity.

In order for the prepared nanocomposites to have excellent properties, the AuNPs should be well dispersed in the matrix without large aggregates and have the smallest possible size distribution of the nanoparticles, as otherwise they reduce the final properties. Therefore, it is important to explore an effective method that is easy to control the size distribution in the cellulose matrix and prevents the formation of aggregates in a large-scale production. [53]

Currently, a large amount of techniques have been developed to attach AuNPs to the cellulose fibers.

2.3.1 Blending of compounds

The mixing of prepared AuNPs and polymers to hybrids by direct deposition has already been reported several times. For instance, Lam et al. first dispersed nanocrystalline cellulose (NCC) in an aqueous poly (diallyldimethylammonium chloride) (PDDA) solution and sonicated to acquire a stable dispersion, generating PDDA-NCC with the use of KNO_3 after drying.[54] Next, the pre-prepared AuNPs were blended with PDDA-NCC under aqueous condition and stirred. After centrifugation

and freeze-drying, the NCC fibers-AuNPs hybrids were prepared. The great advantage of this method is its simplicity, but it easily creates large aggregates that reduce the benefits of AuNPs in the choice of cellulose as a matrix.[53] This process leads to a poor washing fastness if it is used in textiles. In addition, another technique named dip coating, in which AgNPs and AuNPs are applied directly to the cellulose fiber[55,56], is described in detail in the dip coating part of the following section.

2.3.2 In-situ reduction

2.3.2.1With the addition of chemicals

The preparation of cellulose/AuNPs hybrids by in-situ reducing gold salts in cellulose suspensions has been widely employed. The typical idea of this method is to use a soluble gold salt as a precursor and a reducing agent and a co-stabilizer to reduce the gold salt in such a way to form nanoparticles as well as to avoid agglomeration, respectively. So far, the chemical, which has widely been used to reduce metal ions in cellulose matrices, is sodium borohydride.[53,57] Moreover, the use of trisodium citrate and hydrogen has also been reported as reducing agents.[58]

He et al. used lint-free cellulose papers and filter papers as sources of cellulose fibers to synthesize gold nanoparticles. They first prepared an aqueous gold trichloride cellulose (TC) fiber suspension, and then added sodium borohydride to form metallic gold. The size of the obtained gold nanoparticles (<10 nm) was tuned by changing the reaction conditions, such as reaction temperature and the added amount of chemicals. They concluded that the successful synthesis of monodisperse gold nanoparticles could be attributed to the nanoporous structure of cellulose and its high oxygen content (ether oxygen and hydroxyl groups). The oxygen groups are able to stabilize metal ions in the fiber matrix via ion-dipole interactions, while the nanoporous structures allow the access of metal ions, thereby avoiding the aggregation of gold nanoparticles.[57]

In addition to unmodified cellulose, chemically modified cellulose has been utilized as a matrix for the in-situ synthesis of AuNPs.

Methyl cellulose (MC) was prepared by Sahoo and his coworkers to employ it as

a template to prepare cellulose/AuNP hybrids. Hydrogen gas served as the reducing agent when a solution of methyl cellulose was mixed with tetrachloroauric acid. TEM images indicated that spherical gold particles were produced successfully. However, also oval-shaped particles with an average diameter of ~55 nm were observed. As FTIR showed, the MC is not affected by the reaction conditions and the methyl groups were recognized to stabilize the gold nanoparticles physically.[58]

Besides methyl groups, amino-functional groups were also attached onto cellulose fibers to reduce and anchor gold nanoparticles by Boufi et al.[58] The alcohol groups of cellulose were first activated with a dimethylacetamide/ LiCl solution containing N,N′-carbonyldiimidazole (CDI). Afterwards, the mixture was reacted with one of the following three chemicals: 1,4-diaminobutane (DAB), 1,6-di-aminohexane (DAH), or tris(2-aminoethyl) amine (TAEA). Then, the chemically modified fibers were immersed into a $NaAuCl_4$ solution to form gold nanoparticles. The interaction time between the aqueous $NaAuCl_4$ solution and the cellulose determined the size of nanoparticles. With an increase in the reaction time, the size of AuNPs became larger. In this study, they discovered that amino functional groups acted as coordination sites during the synthesis of gold nanoparticles. The particles obtained were chemically anchored on the surface of cellulose to avoid big aggregation, resulting in the stabilization of the hybrid material. The possible reaction mechanism can be described in three steps: After a coordination with the amine groups, the gold ions are reduced to form gold nanoparticles by the unreacted hydroxyl groups of the anhydro glucose units of cellulose, and finally by the growth of the nuclei.[59]

In addition, TEMPO-mediated oxidation was utilized to introduce carboxylate groups onto cellulose to contribute to the mobilization of gold nanoparticles. After mechanical treatment, cellulose nanofibers were separated individually because of the repulsion force between the negatively charged carboxylate ions. The resulting type of fiber displayed excellent mechanical properties with high stiffness, a low thermal expansion coefficient, and low density, due to the presence of highly crystallized regions.

Similarly, tetrachloroauric acid was also involved as a source of gold to generate AuNPs through the reduction effect of sodium borohydride. In this way the carboxylate groups serve as the reaction sites, which immobilize both the gold ions and the gold nanoparticles. Final results indicated that AuNPs were successfully synthesized and were well dispersed on the surface of the cellulose nanofibers. However, in the absence of cellulose as a reduction site, gold nanoparticles would form big aggregates, proving that the carboxylate groups really positively contribute to the complexation of AuNPs.[60]

Another interesting approach for the synthesis of AuNPs is the combination with ionic liquids, which are excellent solvents for cellulose. Yokota and his co-workers initially prepared cellulose-TSC derivatives with the thiosemicarbazide (TSC). The obtained cellulose-TSC were dissolved in 80 wt% NMMO/H_2O, the gold nanoparticles were prepared instantaneously after adding $HAuCl_4$ solution drop-wise. Based on the TEM analysis, the gold nanoparticles were one-layer dispersed with a uniform size of 6.8 ± 1.7 nm without the presence of big aggregates. XPS also proved that a bond between sulfur and gold was formed, which means that the obtained nanoparticles were conjugated with TSC functionalized cellulose.[61]

2.3.2.2Without the addition of chemicals

In order to find a facile and eco-friendly approach to prepare gold nanoparticles, an in-situ method has been optimized to react without the addition of an external reducing or stabilization agent. It has been reported that the porous structure of cellulose offers access to the absorption of Au salts, which can subsequently be reduced to AuNPs by functional groups of cellulose such as the reducing end groups. This implies that the porous structure and the presence of ether and hydroxyl groups in cellulose fibers form an effective nano-reactor for the synthesis of AuNPs. The gold ions are anchored onto the cellulose fibers via ion-dipole interactions, which also stabilize the NPs after their reduction via surface interactions.

Compared to other methods, this process displays considerable advantages. Cellulose macromolecular chains play an important role to improve the AuNPs'

distribution inside the cellulose matrix and they also prevent the formation of aggregates. Moreover, the cellulose chains facilitate the formation of AuNPs with a narrow size distribution and a well-defined shape.[8,57,62]

Johnston and Nilsson utilized lignin-containing cellulose fibers as a substrate to synthesize nanogold and nanosilver composites without any addition of external chemicals making it an entirely green approach. Kraft paper was put into a solution of chloroauric acid to absorb gold ions first, then the Kraft paper treated with Au^{3+} was reacted until no change of color could be observed anymore. SEM images and the change of color indicated the formation of gold nanoparticles. In this study, they proposed that the phenol and aromatic methoxy groups of lignin played a critical role in this reaction as bleached pulp did not show the same results compared to unbleached pulp. They assumed that the interaction of Au^{3+} with negatively charged phenol and methoxy groups enabled the absorption of Au^{3+} on cellulose fibers, whereas the phenol groups adjacent to the methoxy groups had an oxidizing effect similarly to the effect of trisodium citrate[8]. However, the mechanisms was not approved.[8]

Silk as a raw material was also employed for the preparation of gold nanoparticle-cellulose hybrids via a green reduction method by Tang Bin and co-workers. In a similar way as stated before, silk was immersed into a precursor solution to absorb Au^{3+}. Then the silk with Au^{3+} was placed into an oven of 85 ℃. The color of silk and SEM images could approve the formation of gold nanoparticles. The mechanism behind was explained as follows: Silk, which contains many amino and carboxyl groups, could enable the absorption of Au^{3+} through hydrogen bonding, which could subsequently be reduced by the remaining amino and carboxyl groups to form Au nanoparticles. In addition, they found that the addition of chemicals could improve the colorfastness of silk compared to the approach discussed before.[10]

2.3.3 Dip coating

Cellulose-AuNPs complexes can be applied in surface enhanced Raman scattering (SERS), to assist the analysis of organic molecules on sample surfaces. SERS applies

a common optical phenomenon composed of two phases. The first one is to improve the local electromagnetic field due to the localized surface plasmon. Secondly, a resonant charge transfer between the molecule and the metal surface will be enhanced obviously.[63]

Dip coating has been utilized to form cellulose-AuNPs hybrids for SERS. In this method, the AuNPs are synthesized and stabilized firstly in an aqueous solution by the reduction method mentioned before. Then a drop of AuNPs solution is placed on the surface of the cellulose fiber or film and the water is waited to evaporate to leave AuNPs. With this method, maintaining the same degree of aggregation on the cellulose paper is however challenging. Afterwards, they found that the initial packing density of AuNPs in solution was retained on the paper matching the degree of aggregation. It was reported that the SERS intensities were positively related to the concentration of AuNPs, as the SERS properties improved with an increased concentration. The mechanism behind is the existence of an inter-particle plasmon coupling of gold nanoparticles, which can dramatically enhance the electromagnetic field intensifying the SERS signal. Meanwhile, compared to AuNP-silica, AuNPs coated cellulose paper performs more efficiently regarding the enhancement factor of SERS. Moreover, AuNPs-treated fiber paper showed the most reproducible and sensitive SERS signals among all of substrates. This is because the bulky molecules of paper are able to amplify the SERS signal and result in the formation of a decent structure, which allows an enhanced layer plasmon coupling to occur (interlayer enhancement).[63]

For example, Zhang et al. assembled AuNPs onto the surface of cellulose nanofibers using a dip coating method. The nanofibers were prepared by ball milling from a softwood source. And the AuNPs were synthesized and stabilized by reduction through citrate. Their final output indicated that the cellulose-AuNPs material prepared by this method was able to enhance the SERS signal significantly due to the presence of gold nanoparticles. Furthermore, they found that using nano-cellulose as a substrate can achieve a higher reproducibility than using paper and silica since the roughness of nano-cellulose fibers can be focused better under the microscope.[64]

2.4 Applications

2.4.1 Recycling of metals in water

In accordance with industrial development, the recovery of metals from waste water has gained more and more attention in respect of sustainable and green chemistry. In 2012, cellulose was chosen to be used as a substrate to absorb and recycle gold from waste water by Gurung *et al.* They first combined epichlorohydrine (ECH) or H_2SO_4 with cellulose through cross-linking. Followed by that, N-aminoguanidine (NA) was used to donate a functional group for the absorption of metal nanoparticles. Applying the surface of unmodified cellulose as a reference, they found that the modified cellulose complex absorbed metal nanoparticles very well, while the unmodified cellulose could not absorb any metal nanoparticles. Meanwhile, the absorption efficiency of three types of metal particles (Au, Pt, Pd) was studied in this paper. Pd showed similar behavior to Au, which was higher than for Pt. In comparison with ECH-NA-cellulose, Sulf-NA-cellulose showed a superior performance with respect to metal absorption. The result proved that rising the concentration of metals did had no effect on the final output. Interestingly, Gurung *et al.* also employed base metals to carry out the same experiment. No matter whether choosing ECH-NA-cellulose or Sulf-NA-cellulose, no base metal was absorbed. The proposed mechanism assumes that anion exchange provides access to Au ions bound to the functional groups anchored by electrostatic effects. Base metals possess cationic properties in this state, which is why they have not been adsorbed. Materials pretreated with sulfuric acid show a better absorption because the sulfuric acid destroys part of the crystalline regions of cellulose and thus creates more reaction sites. In addition, the absorbed gold ions are reduced to gold metals. SA-NA-cellulose could therefore be used for the recycling and reproduction of noble metals in waste water and industrial waste.[64]

2.4.2 UV-protection

Ultraviolet (UV) radiation is the most common cause of skin cancer, which is why the development of sun protection clothing has become an important health issue. Today there are three common approaches applied for the production of UV-protective fabrics: the novel fabric structure, denier, and the addition of chemicals (e.g. oxybenzones).

Cellulose-based fibers coated with gold nanoparticles have already proven to provide excellent UV protection properties with low use of chemicals. Tang and his co-workers in-situ synthesized AuNPs on the surface of silk fabrics to yield UV-blocking features.[10] First of all, they immersed silk fabrics into the aqueous $HAuCl_4$ solution to react under certain reaction conditions. After acquiring samples, they mainly tested the transmittance values (UVA&UVB) and the UV protection factor (UPF). The measurements indicated that the average transmittance values of AuNPs coated silk fabrics decreased dramatically compared to the original fabric. And with the increase in the concentration of AuNPs, the transmittance values tended to decrease. However, when the gold content reached the threshold, the transmittance values remained constant. In terms of UPF, the values of the coated silk were three to seven times higher than those of pure silk and were between100-170. According to the standard of AATCC, if the UPF is above 97, the UV protection properties of the fabric can be classified as excellent.[10]

Furthermore, Zheng *et al.* coated cotton and silk with gold nanorods instead of spherical gold nanoparticles. In this way, they primarily prepared gold nanorods solutions with different aspect ratios through a seed-mediated approach. Subsequently, the cotton and silk fabric pieces were dipped into the previous aqueous solution at 45 ℃ for 4h. Samples were then taken and rinsed with water to dry overnight and perform measurements. It was reported by Zheng et al. that the average transmittance values in the UVA (315–400 nm) and UVB (280–315 nm) regions of the coated fabrics decreased, which means that a part of the UV light was blocked when passing through these fabrics.

Furthermore, the UPF value improved significantly to 6.13-41.3 for cotton and 8.6-32.1 for silk. Based on the ASTMD 6603, these UPF values can be categorized as excellent and very good for UV protection. [11]

In a word: cellulose-AuNPs materials have excellent UV protection properties, making them promising candidates for sun protection clothing and medical applications.

2.4.3 Anti-bacterial properties

Combining various agents with cellulose fibers to obtain anti-bacterial properties has gained considerable interest in biomedicine. Nowadays, with the increasing exploration of nanoscale particles with unique chemical and physical properties, different types of inorganic nanoparticles have been studied. Among them, AgNPs show the most dominant anti-bacterial properties, but their low biocompatibility still limits their applications.

Compared to AgNPs, AuNPs have become promising candidates in interaction with cellulose due to their high biocompatibility and non-toxicity. Tang et al. successfully confirmed these properties with AuNPs coated silk fabrics.[10] They completely inhibited the growth of gram negative bacteria, E. coli. In addition to Gram-negative bacteria, AuNPs-cellulose hybrids show an inhibition activity for the Gram-positive bacteria S. aureus, as shown by Zheng and his fellows.[11]

The mechanism of bacterial growth inhibition by AuNPs is intended to destroy the integrity of cell membranes through electrostatic interactions with the AuNPs. The membrane potential is affected, which inhibits the ATP reaction in the cells, reduces the energy transfer and hinders the binding of t-RNA. As a result, bacterial cells can no longer proliferate and cause cell death.[65]

Research questions

As already mentioned, only unbleached wood pulp was used as substrate in the in-situ reduction. It implies that the raw materials have their own color, which can create barriers in matching the final color of textile due to the interference of the original colors. In addition, the gold nanoparticles are coated onto the textile through electrostatic effects, which are relatively weak bonding forces, causing the attached AuNPs to be unstable.

In this master thesis I will therefore try to answer the following research questions:

1. Is it possible to use bleached pulp as a raw material for the production of AuNPs using the in-situ reduction approach?
2. How to improve the affinity between AuNPs and textiles for commercial use?
3. What are the effects of the pH of the solvent and the addition of CTAB on the formation of AuNPs?
4. Does the addition of AuNPs alter the mechanical properties of the Ioncell fibers?

3. Experimental

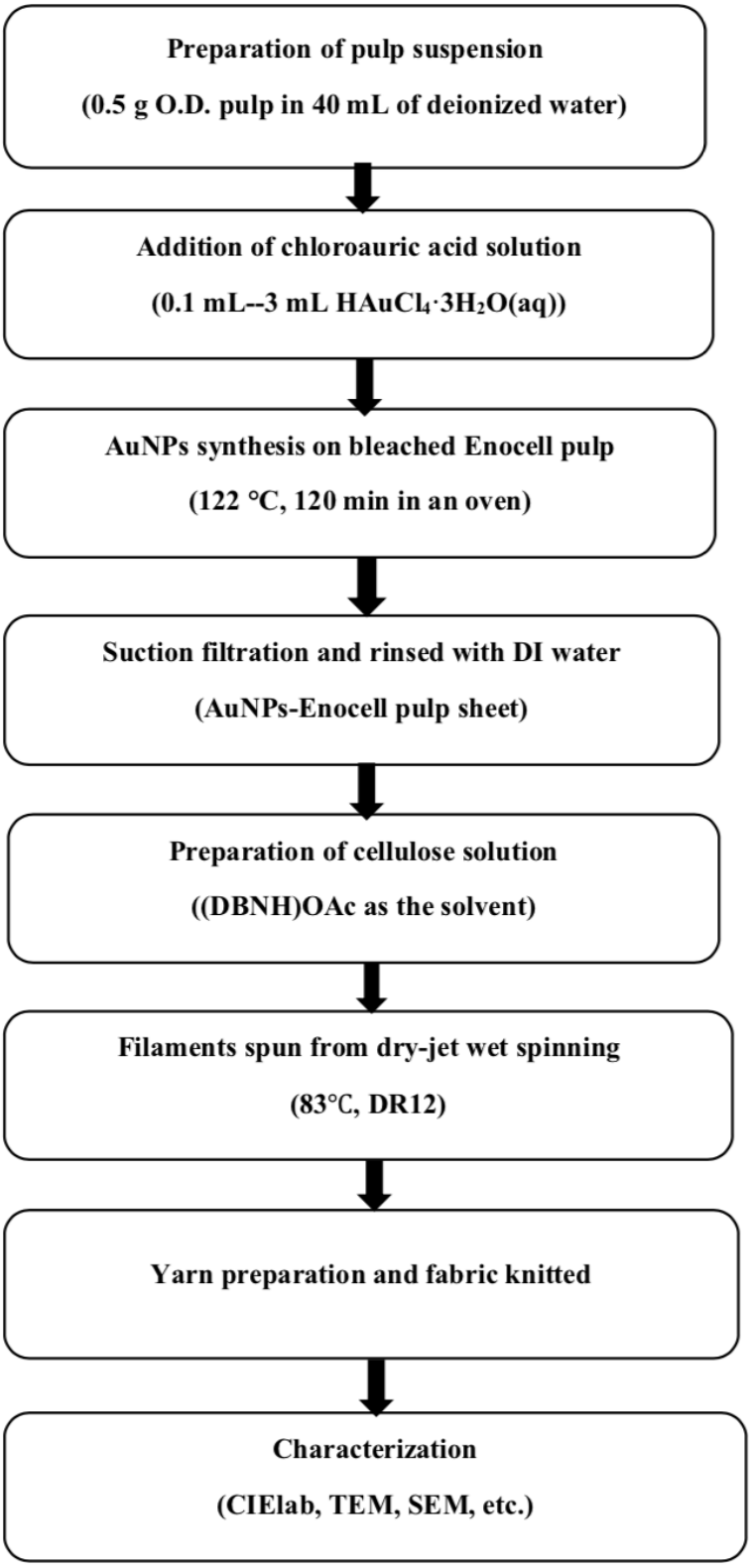

Figure 4. Flow chart of the overall procedure

3.1 Materials

Enocell birch pre-hydrolyzed kraft pulp (PHK) 476 ml g^{-1} (Mw = 274.3 kg mol^{-1}, Mn= 68.2 kg mol^{-1}, PDI = 4, xylan content:5.3%, cellulose content: 94.3% from Stora Enso, Finland), 1,5-Diazabicyclo[4.3.0]non-5-ene (DBN, 99 %, Fluorochem, UK), acetic acid (glacial, 100%, Merck, Germany), Hexadecyltrimethylammonium bromide(CTAB, 96%, Sigma, USA), Gold chloride trihydrate($HAuCl_4$, 99%, Sigma, USA), Silver nitrate($AgNO_3$,99%, Sigma,USA).

3.2 The preparation of AuNP-Enocell pulp

Small batch (0.5 g pulp)

The chloroauric acid solution (50mM) was prepared firstly for the synthesis of gold nanoparticles.

Before starting the in-situ synthesis of gold nanoparticles, the pulp (Enocell) should be exposed to air overnight to enable a homogenous dry matter content.

0.5g of oven-dried (O.D.) pulp was added to 40mL of water, and the mixture was then mixed vigorously by magnetic stirring for 15mins to ensure the pulp to be completely dispersed. After that, a certain amount of chloroauric acid solution (50mM) was dropped into the pulp suspension and mixed for 5mins. The resulting slurry was transferred to wild-neck bottles with caps and was placed into a 122 ℃ oven for 2h to allow the synthesis of gold nanoparticles. When closing the caps of the bottles, it is dangerous to screw them completely since the evolving pressure could make them burst. The right way was to cover the neck of the bottles loosely to prevent major water evaporation, thereby forming gold nanoparticles homogeneously on the surface of pulp.

After 2h, the previously colorless pulp suspension changed to pink or purple according to the different recipes. Once the color is stable, this means that the reaction is complete. The bottles were taken out and cooled down in the ice water for suction filtration. AuNPs-Enocell pulp was then filtrated with a 200 mesh filter paper and rinsed

with deionized water for three times, forming a wet pulp sheet. Then this sheet was collected for CIELab measurement after drying at 45℃ overnight.

Big batch (5-10g pulp)

When preparing a big batch with 10g of pulp, the volume of water should be calculated based on the liquor-to-pulp ratio of 80:1. It is better to choose glassware of 1000mL with a wide bottom. Otherwise, the slurry cannot boil and achieve the required temperature. To ensure efficient mixing, the slurry has to be stirred by glass bar every 10 minutes.

3.3 Effects of reaction conditions

In this work, a couple of influencing factors were explored including the wt% of Au/pulp, the pH of the dispersion, the addition of silver ions, the addition order of chemicals, and CTAB.

3.3.1 Amount of Au^{3+}

A range of different wt% of Au^{+} to Enocell was tested when the remaining test conditions were kept constant (Table 1). The Au content is shown on the basis of the weight ratio of Au^{3+} and Enocell pulp. The calculation process is explained in the appendix using the example of the first recipe from Table1.

Table 1. (wt%) of Au^{+} in the composite

Number	Enocell pulp(g)	Volume of added CA(mL)	mol of added CA	Mmol of added CA	mass of added CA(g)	mass of Au3+(g)	Au^{3+}/pulp (wt%)
1	0,5	0,3	0,000015	0,015	0,00591	0,00295	0.59
2	0,5	0,2	0,00001	0,01	0,00394	0,00197	0.39
3	0,5	0,15	0,0000075	0,0075	0,00295	0,00148	0.30
4	0,5	0,1	0,000005	0,005	0,00197	0,00098	0.20
5	0,5	0,08	0,000004	0,004	0,00158	0,00079	0.16
6	0,5	0,05	0,0000025	0,0025	0,00098	0,00049	0,10
7	0,5	0,03	0,0000015	0,0015	0,00059	0,00030	0,06
8	0,5	0,01	0,0000005	0,0005	0,00020	0,00010	0,02

3.3.2 pH

In this experiment, water was replaced with solutions with different pH values. These solutions were prepared by adding either HCl or NaOH. The recipe is illustrated in Table 2.

Table 2. A series of experiments of various pH

Number	pH	Volume of added 50mM CA(mL)	Enocell pulp(g)
1	2,03	0,3	0,5
2	2,75	0,3	0,5
3	5,07	0,3	0,5
4	6,57(water)	0,3	0,5
5	9,92	0,3	0,5
6	10,53	0,3	0,5
7	12,02	0,3	0,5
8	13,5	0,3	0,5

3.3.3 The addition of Ag ions

In this part, $HAuCl_4$ was replaced with $AgNO_3$ to generate AgNPs in the matrix of cellulose by using the same operation as in the previous section. Besides, a variety of ratios of Ag^{+}/Au^{3+} was also tested in this experiment. The recipe is demonstrated ratios of Ag^{+}/Au^{3+} was also tested in this experiment. The recipe is demonstrated in table3.

Table 3. Different Ag^{+} and Au^{3+} concentrations applied on Enocell pulp

NO.	Enocell pulp(g)	Volume of added 50mM CA(mL)	Volume of added 50mM AgNO3(mL)	Ratio(Ag^{+}:Au^{+})
1	0,5	0	0,05	N.A
2	0,5	0	0,03	N.A
3	0,5	0,01	0,04	4:1
4	0,5	0,01	0,02	2:1
5	0,5	0,015	0,015	1:1
6	0,5	0,02	0,01	1:2
7	0,5	0,025	0,005	1:5

3.3.4 The order of addition of Ag^{+} and Au^{3+}

We conducted two pairs of control groups concerning this factor. First Ag or Au ions were added, then the other chemicals were charged. The specified information is included in Table 4.

Table 4. Recipe regarding the addition order of Ag^{+} and Au^{3+}

NO.	Pulp(g)	water(mL)	50mM $HAuCl_4$(mL)	50mM $AgNO_3$(μL)
Adding Ag firstly and after Au				
1	0,5	40	0,02	0,01
2	0,5	40	0,01	0,02
Adding Au firstly and after Ag				
3	0,5	40	0,02	0,01
4	0,5	40	0,01	0,02

3.3.5 The addition of CTAB

In the traditional seed-mediated method for the preparation of AuNPs, cetyltrimethylammonium bromide (CTAB) plays an essential role in shaping and stabilizing the nanoparticles. Here, the addition of CTAB was designed to verify whether it could show the same role in this green method. The exact formula is reported in Table 5.

Table 5. Recipes for the addition of CTAB

Sample	pulp (g)	water(mL)	50mM CTAB(mL)	50mM CA(mL)
1	0,5	30	10	0,03
2	0,5	33	7	0,03
3	0,5	35	5	0,03
4	0,5	38	2	0,03

3.4 The production of regenerated Au-NP Inocell fibers

The resulting Au-NP pulp was utilized as a raw material to regenerate fibers via dry-jet wet spinning. Briefly, the (impregnated) pulp was dissolved in ionic liquid (DBNH] OAc) at 80 ℃ under reduced pressure to prepare a cellulose solution which is referred to as dope. The dope is then spun to textile grade staple fibers by dry-jet wet spinning.[26]

3.4.1 Preparation of [DBNH]OAc

DBN was used to neutralize acetic acid to prepare [DBNH]OAc. An equimolar amount of acetic acid was slowly poured into DBN under permanent cooling due to the exothermic nature of the reaction. Then the resulting solution was stirred for 1h at 80 ℃.

3.4.2 Dope preparation

To ensure that the AuNPs-Enocell pulp could be dissolved in the IL, it had to be ground by a Wiley Mill to become a powder.

As reported before by our lab, 13% (pulp/IL) was the best option for spinning. Using this concentration, it is possible to acquire fibers, prepared with a draw ratio (DR) of 12. This DR is required to produce staple fibers with a titer of 1.3 dtex (diameter approx. 10μm), which is the standard fiber thickness for processing into textile yarns.. Additionally, these Ioncell fibers possessed excellent mechanical properties compared to Viscose fibers.

Therefore, the oven dry (o.d.) AuNPs-Enocell pulp and IL were put into a reactor

in a ratio to obtain a cellulose concentration in the resulting dope of 13%. Before dissolution, the mixture should be mixed by hand until big particles and aggregates of cellulose disappear. Reaction took place for 80mins under reduced pressure with stirring. After dissolution, a violet dope was obtained and filtrated at 80 ℃ to remove undissolved cellulose particles and ensure uniform solution quality. Finally, the filtrated dope was shaped to fit the size of the spinning device, and wrapped by Parafilm to store at 5-7 ℃ for a few days for solidification.

3.4.3 Dry-jet wet spinning

Before spinning, the rheology of the dope should be measured to find the most suitable spinning temperature.

The solidified dope was first inserted into the cylinder（Fourne Polymertechnik, Germany). Multi-filaments were spun from a 200-hole spinneret, holes' diameter 0.1 mm, at 83 ℃ extruded by a piston, passing through a 1 cm air-gap into a water coagulation bath. It should be noted that the immersion depth to the first deflection roller, the deflection angle and the retention distance of the filament bundle were kept constant. As mentioned above, a draw ratio (DR) of 12 was adjusted. The calculation of the DR is shown in the equation below. [66]

$$D_r = \frac{V_{tu}}{V_e}$$

Where, V_e represents the extrusion velocity, V_{tu} stands for the take-up velocity of the godet couple

3.4.4 Fiber opening, washing and finishing

After spinning, the fibers were cut into 4 cm staple fibers. These shorter filaments were then first opened by hand. The opened filaments were washed in a 80 ℃ water bath for 2 hours to remove the residual ionic liquid. After two days, the stress-strain behavior of the conditioned fibers was measured. In addition, the staple fibers were spin finished to improve the run ability of yarn spinning by reducing the surface energy.

First of all, according to the weight of the fibers, the amount of water and chemicals (Leomin&Afilan, bought from Archroma) required was calculated. Then, the chemicals were added into the 50 ℃ water and stirred until they dissolve entirely. Followed by that, the fibers were placed in this solution to immerse for 5mins. Lastly, the fibers were dried at room temperature and fully opened by a Mesdanlab fiber opener.

3.5 Yarn and fabric making

3.5.1 Yarn making

This process was performed by DirectTwist® (cone-to-cone multifunction twisting machine), Agteks, Istanbul, Turkey.

Carding: The opened fibers were aligned parallel to each other to produce a thin web of fiber fleece. As it moves, it can produce a rope-like strand of parallel fibers after passing through a funnel-shaped device.

Combing: To ensure that the yarn is smoother and finer, the short fibers would be removed from strand.

Drawing out: The sliver was first elongated under a series of rollers rotating at different speeds to form a single, more uniform strand. The strand is then fed into large cans with a small amount of twist.

Twisting: In this stage, the strands of fiber are further elongated and twisted. These fibers are called the roving.

Spinning: The roving is elongated by roller and passed through the eyelet. Then spindle turns the bobbin at a constant speed. This turning of the bobbin and the movement of the traveler twists and winds the yarn in one operation.

3.5.2 Nonwovens sample preparation

In this study, nonwoven samples were prepared by a mechanical web formation process (Automatex, Italy). The opened fibers formed randomly oriented nonwovens

with roll cards that convert fibers into the surface. In this step, a Batt drafter was used to increase the delivery speed of the web. The resulting web was then bonded by needle punching, with the aim of consolidating and compacting the webs by repeatedly insertion barbed needles into the web. The prepared samples were utilized for the anti-bacterial measurement.

3.5.3 Knitted sample

Three similar threads were plied together. The single threads show Z-twist and 700 twist/m. The plying twist was S and 300 twist/m. The yarn was knitted by a lab-scale circular knitting machine (L. Degoisey Tricolab ITF DS 34, France). The structure was single jersey.

3.6 Characterization

3.6.1 AuNPs Enocell pulp

3.6.1.1 CIELab

After drying overnight, the pulp was collected for measuring reflectance spectra within the range of visible light and the **L**, **a**, **b** values were determined by a Gretag Macbeth spectrometer, with a standard illuminant D65 and a CIE10 ℃ observer. Pulp sheets were pressed by glass plate to make the surface as uniform as possible to avoid interferences caused by the roughness of the surfaces. Each sample was measured for ten times and the mean values were calculated.

After getting the reflectance spectrum, it is better to convert it into an absorption spectrum based on a formula.

3.6.1.2 Transmission electron microscopy (TEM)

0.01g pulp coated with AuNPs was weighed into a 20 mL glass bottle, then 9mL deionized water was added and the mixture was shaken vigorously until the pulp dispersed completely. Then the resulting suspension was treated in an ultrasonic bath for 20mins in order to break up significant aggregation of the nanoparticles on the pulp

surface. Then drop 5μL of resulting dispersion were transferred on a copper grid immediately and it was waited for 5 min for the substance to absorb onto the grid surface. Finally, filter paper was used to remove extra water from the edges and the copper grid with the sample was put into a storage box to dry for ten minutes. When doing this, it was crucial to confirm that every tool was clean as already little contamination would ruin the samples. Therefore, for each sample duplicates should be measured. The imaging was performed by JSOL Tencial microscope at 120kV.

3.6.1.3 Gel permeation chromatography (GPC) measurement

The GPC-system consisted of a pre-column (PLgel Mixed-A, 7.5*50 mm), four analytical columns (4*PLgel Mixed- A, 7.5*300 mm) and a RI-detector (Shodex RI-101). The samples were prepared as follows. After weighing around 50mg of virgin and Au treated Enocell pulp into filter tubes, the tubes were inserted into vacant ports in a vacuum manifold. Then 4 mL of Milli-quality water was dropped into the tubes to activate the cellulose overnight. Then water was removed by vacuum, and then 2mL of acetone was added and removed by vacuum to eliminate possible retained water. Thereafter, the pulp was activated overnight with the addition of 4mL of acetone. The tubes were emptied again and filled with 4 mL of pure DMAc, keeping the condition for overnight. DMAc was removed as before; the residue was mixed with 5.0 mL of 90 g/l LiCl/DMAc at room temperature under a constant slow speed magnetic stirring to prepare a solution with the concentration of 10 mg/mL. 0.5 mL of sample was taken and diluted with 4.5mL of pure DMAc. After stirring, 2mL of the resulting solution was taken out and filtered to be prepared for the GPC analysis. A volume of 100ml was separated at 25℃ at a flow rate of 0.750 ml/ min with 9 g/l LiCl/DMAc as eluent. Pullulan standards with molecular weights ranging from 343 Da to 708,000 Da were selected for the calibration. A correction of the molar mass distribution obtained by direct-standard-calibration was done with an algorithm calculating cellulose-equivalent molar masses of pullulan standards ($MM_{Cellulose} = q * MM_{Pollulan}^{P}$,with q =12.19 and p=0.78).This testing was conducted referencing the method reported by L. Wise.[67]

3.6.2 AuNPs-Ioncell fibers

3.6.2.1 CIELab

The whole process was similar to the operation for Enocell pulp, but the fibers should be ground before the measurement. After washing and drying, the filaments were ground by a small Wiley mill to form a powder. 0.5g powder were then mixed with 40mL of deionized water to obtain a flat filter cake after filtration.

3.6.2.2 Tensile testing

Through fiber testing, the mechanical properties of AuNPs-Ioncell fibers were determined, including diameter, tenacity, and elongation at break under conditioned (23℃, 50% relative humidity) and wet states. Before carrying on this testing, the fibers should be placed in a conditioned room for overnight. This testing was performed by using a Vibroskop 400 and Vibrodyn 400 (Lenzing Instruments GmbH & Co KG, Austria) the gauge length was 20mm, pretension 100mg and the speed 200mm/min.

3.6.2.3 SEM-BD

Here, cross-section samples were also prepared for SEM (Phenom Prox, back scattered mode). The fibers were taped into aluminum cups. After adding deionized water, these cups with fibers were placed into a freezer overnight. The resulting frozen samples were immersed in liquid nitrogen for 5 mins, then cracked in the center to gain the cross sections of fibers through cryo fracture. After drying for overnight, the cross-section samples were placed onto a SEM holder.

3.6.3 Yarns

Similar to the filaments, tensile testing was applied to the yarn. First of all, the hank composed of 10 skeins was weighed to calculate the Tex value. Then this hank was separated into one by one in the length of 1meter. Picking up the most homogeneous part with distance of 25CM on skeins after weighing the mass, and marking it for the following measurement. Each one of skeins were attached to one paperboard to avoid twisting and conditioned overnight. In this experiment, the device used was MTS 400 tensile tester using 50N load cell, 250 mm gauge length and 250mm/min of speed. In

order to guarantee the accuracy, this tensile testing of yarn was performed for 30 times and use the average value.

3.6.4 AuNP-Inocell fabric sample

3.6.4.1 UV-Protection

The UV-blocking properties of uncoated and Au-NPs coated fibers were measured according to the standard SFS-EN 13758-1:2001. After assembling the knitted samples on a holder, the transmittance between 290nm and 400nm was recorded. The measurements were conducted ten times and the mean value was used as the final result.

3.6.4.2 Washing fastness properties

The washing fastness of the AuNP-Inocell fabric samples was evaluated according to the ISO 105-C06:2010 standard. The fabric was cut into one specimen measuring 100mm*40mm and was attached to a multi-fiber adjacent fabric next to the face side. Then the prepared sample was put into a stainless steel container containing 150mL detergent solution (1/250 g/mL) and 10 steel balls were added under 40 ℃. After the washing machine was warmed up to 40 ℃, the containers with the samples were inserted and the machine was operated for 40 mins at the same temperature. Followed by that, the composite specimen were rinsed by two separate 100mL portions of water at 40 ℃ extracting the excess water from the composite specimen. Finally, the specimen were dried in air below 60 ℃. The CIELab value was measured before and after washing to indicate the stability of color against washing.

4. Results and discussion

4.1 Coloring of fibers to generate AuNPs

The green method for the in-situ synthesis of gold nanoparticles using a cellulose matrix as a reactor has been reported before for wool and silk fibers. This work, however, was the first one to use bleached birch pulp as a raw material.

Herein, a green and facile method of in-situ synthesizing Au-NPs in the matrix of bleached birch pulp is demonstrated. As described in the experimental part, after the addition of 50Mm of chloroauric acid to a pulp slurry, the color of the pulp changed progressively from white to pink or purple depending on the concentration of Au^{3+}. This color was caused by the localized plasmon resonance of gold nanoparticles originating from the reduction of Au^{3+} to Au (0), implying a direct synthesis of gold nanoparticles. A series of different colors after washing and drying is shown in Figure 5. And the UV absorption spectra are plotted in Figure 6.

Figure 5. Photography of Enocell pulp treated with AuNPs
(from left to right: 0.59, 0.39, 0.3, 0.2, 0.16, 0.1, 0.06, 0.02 wt%)

To verify the formation of AuNPs, AuNPs coated pulp and a blank Enocell sample were characterized by a UV-Vis spectrometer to obtain a reflectance spectrum. As shown in Figure 6, there was a plasmon resonance band produced at 520-550nm, which proved the presence of AuNPs on the surface of Enocell pulp under this procedure.[39] With an increasing amount of CA, the position of peak rose gradually and the shape of the signal became sharper and sharper. Hence, it can be concluded that the yield of gold nanoparticles with narrow size distribution would increase with increasing amount of CA. Interestingly, the spectrum showed a blue shift inferring that the average size of

AuNPs synthesized on the Enocell pulp became smaller with an increasing concentration. In addition, when the wt% of Au/pulp was higher than 2.95wt%, the Enocell pulp maintained its white color and implying that there was no formation of gold nanoparticles on the pulp. Assumingly, adding an excessive amount of Au^{3+} compared to the number of activation sites on the pulp results in a reaction of Au^{3+} with the prepared AuNPs converting them into Au^{1+} (colorless).

However, Johnston et al. reported that bleached wood pulp showed a lower effectiveness in comparison to unbleached wood pulp in the aspect of synthesizing and anchoring gold nanoparticles. It can be explained that the lignin present in unbleached wood pulp has aromatic methoxy and phenol groups, which were able to facilitate the reduction of gold ions.[8]

Nevertheless, the AuNPs were successfully prepared using bleached birch pulp (lignin-free) as a raw material. Most likely, the large amount of electron-rich hydroxyl groups on cellulose contribute to the reduction of gold ions. After dispersing for a long while, most of the hydroxyl groups are exposed and able to coordinate Au^{3+} ions. The high reaction temperature reduces the energy barrier of reaction activation, thereby enabling the reduction to take place on the sites of the hemiacetal groups to form AuNPs. Subsequently, the formed AuNPs were immobilized on the surface of cellulose avoiding aggregation, which is a phenomenon caused by the high surface energy of Au NPs. It makes the nanoparticles interact with the oxygen-containing groups (–COO−, –OH) on the surface of cellulose anchoring the AuNPs by complexation or electrostatic interactions.[68] Wu reported that the zeta potential of cellulose was around -19mV, showing cellulose to be negatively charged,[66] whereas Au NPs are usually positively charged. Therefore, AuNPs have the capability of combining with cellulose by electrostatic forces. Accordingly, cellulose itself fulfills the requirements of both reducing and stabilizing agents simultaneously. This mechanism can thus support the in-situ synthesis of AuNPs on cellulose without other additives.

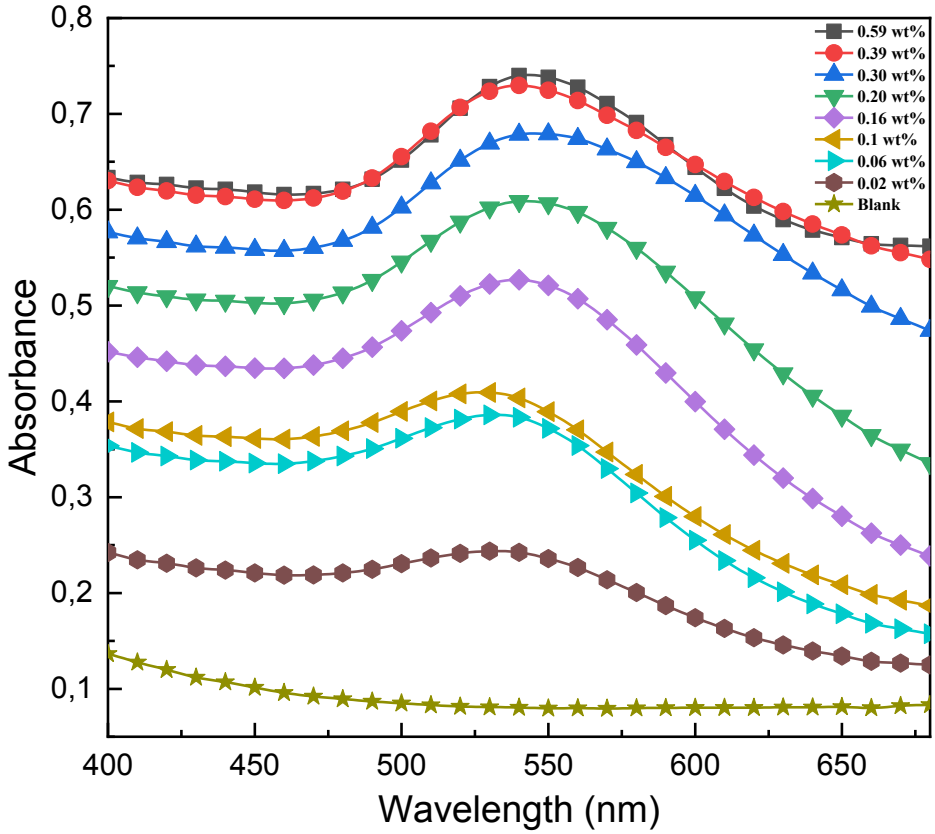

Figure 6. Absorbance spectrum of Enocell pulp treated with different amounts of AuNPs

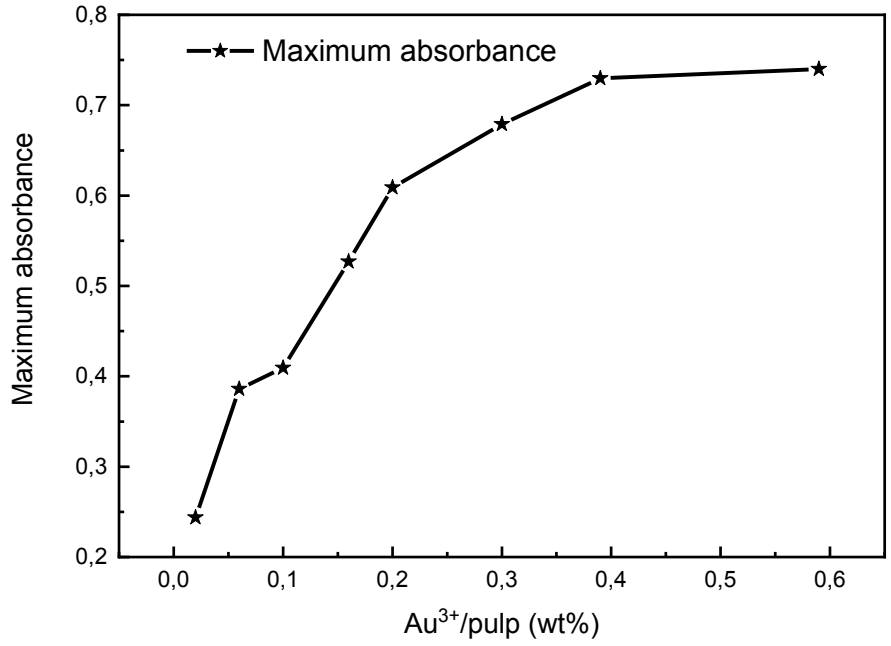

Figure 7. Trend line of maximum absorbance of plasmon resonance bands

In addition, AuNPs are like the chromophores due to the LSPR effect. Reflectance

values **L**, **a**, **b** were hence measured to prove the formation of gold nanoparticles. Here **L** denotes lightness, positive and negative **a** values describe the redness and greenness of the samples, positive and negative **b** values represent the yellowness and blueness attributes. As described in the table 6, the color of the uncoated pulp was white, with a comparatively high brightness **L** value and nearly zero **a** and **b** values. **L** value of all pulp treated with AuNPs decreased and **a** value increased in proportion to the addition amount of CA, comparing with the untreated one. These changes complementally implied the formation of AuNPs with violate color.

Table 6. Reflectance value of samples with different wt% Au^3

Au^{3+}/pulp (wt%)	0,59	0,39	0,30	0,20	0,16	0,1	0,06	0,02	Blank
L	52,781	52,968	55,407	59,961	65,37	72,702	74,284	82,468	92,92
a	6,766	6,498	6,203	9,542	11,856	11,353	11,893	6,543	-0,958
b	-5,462	-5,661	-6,606	-4,393	-2,35	1,852	1,558	1,282	2,797

4.2 Effects of reaction conditions

4.2.1 pH

It is generally known that the reactivity of cellulose is pH-dependent, as the charge of its functional groups, including hydroxyl groups and phenol groups, are affected by different pH conditions. Hence, it is crucial and necessary to explore this parameter in this research. As illustrated in figure 8, experimental conditions with a pH ranging from 2 to 12 have been studied. The overall trend showed a normal distribution, a maximum absorption was achieved under neutral pH. Under acidic or alkaline conditions, the peak value of the plasmon resonance band displayed a decreasing trend until reaching a minimum value at pH 2 and pH 12.2, respectively. This indicates that a neutral pH represents the optimum condition for preparing Au-cellulose hybrids using bleached birch pulp as substrate. However, it is interesting to note that the reduction rate of AuNPs on the Enocell under pH 2 and pH 12 is higher than when monitoring the entire reaction process with neutral solution (The images are shown in the appendix).

Therefore, acquired conclusion can be drawn: The strong acidic and alkaline

environment were able to accelerate the rate of reaction but reduced the yield of gold nanoparticles. Our hypothesis is that cellulose activation is boosted under strong acid or alkaline conditions, at the same time parts of the cellulose structure are deteriorated. It has been demonstrated that the intramolecular hydrogen bonds between C3 and C6 of the anhydroglucose units of cellulose are broken under strong alkaline conditions and high temperatures. [69]

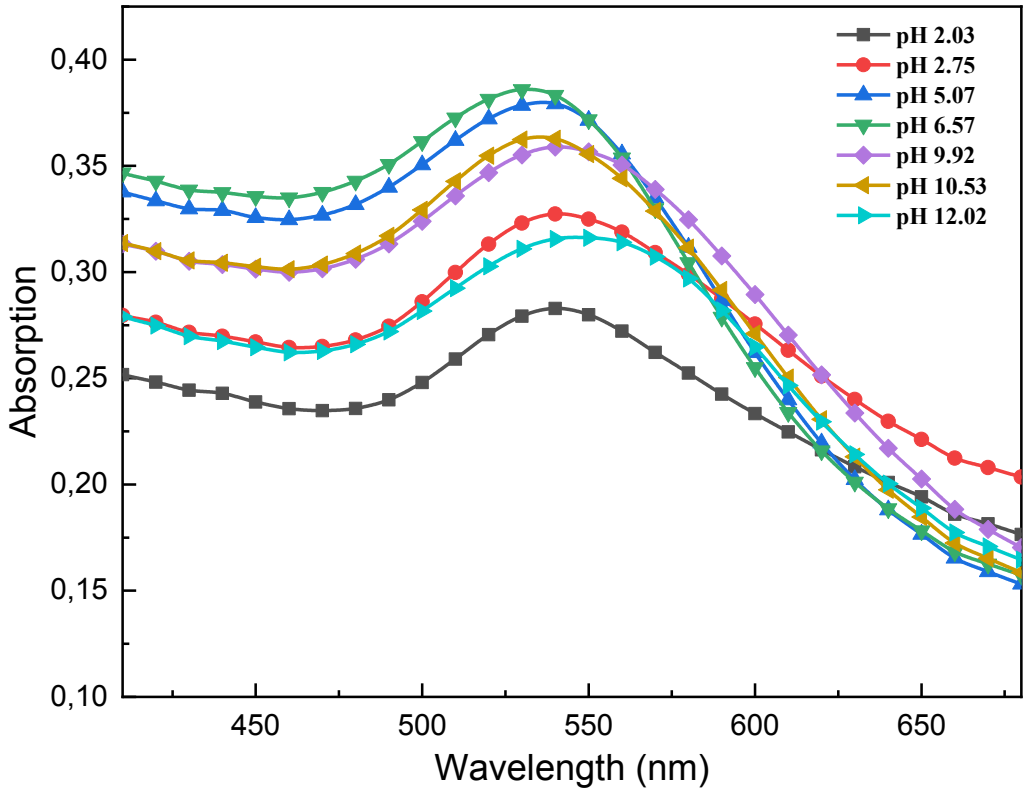

Figure 8. Absorption spectrum of AuNPs-Enocell pulp at different pH conditions (Au^{3+} 0.06 wt%; 1.5μmol)

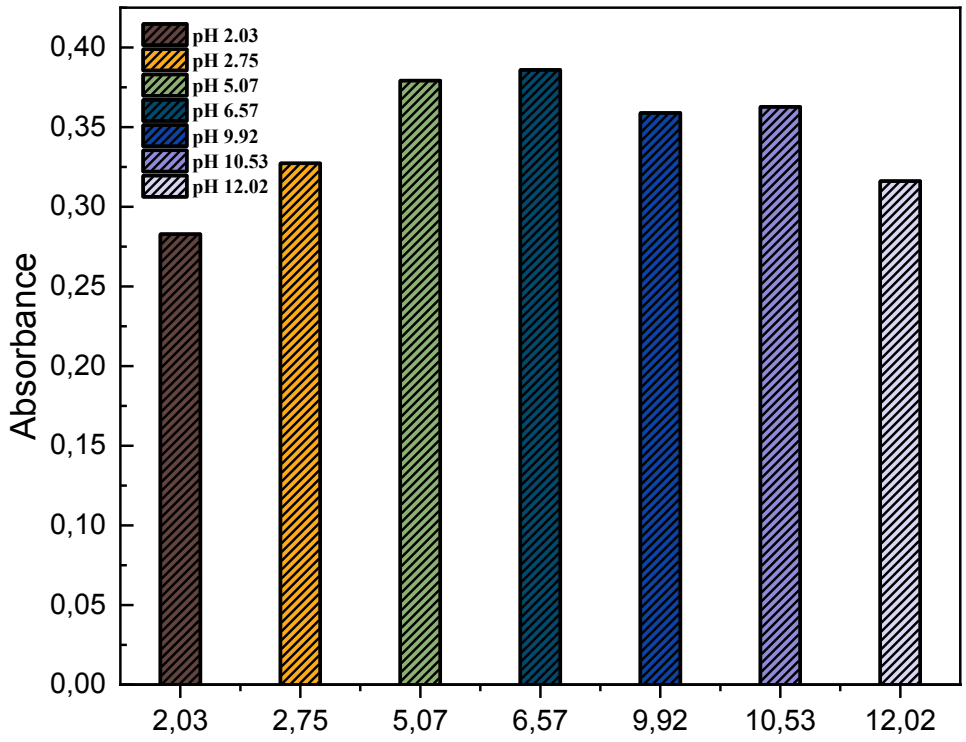

Figure 9. Maximum absorbance of samples prepared at different pH values (Au^{3+} of 0.06wt%; 1.5μmol)

Table 7. Reflectance value of samples prepared under different pH condition (Au^{3+} of 0.06wt%; 1.5 μmol)

pH	2,03	2,75	5,07	6,57	9,92	10,53	12,02
L	79,363	76,399	74,362	74,284	74,589	74,939	77,037
a	4,498	5,279	11,193	11,893	7,586	9,459	5,928
b	-1,811	-3,269	0,529	1,558	-2,081	-1,308	-2,458

4.2.2 Addition of silver ions

Furthermore, we could show that this in-situ reduction could be applied to silver ions on Enocell pulp. After the same procedure and reaction for 2h at 122 ℃, the color of the pulp changed to yellow from the original white, indicating the formation of AgNPs on the pulp surface. In the absorbance spectrum, the LSPR band caused by AgNPs was detected at around 450nm, which is similar to the literature.[68] Besides, the colors and reflectance spectra produced by two different concentrations of $AgNO_3$ (0.2wt%, 1.5μmol; 0.32wt%, 2.5μmol) were almost the same, suggesting that the addition amount did not significantly affect the formation of AgNPs in terms of yield

and size.

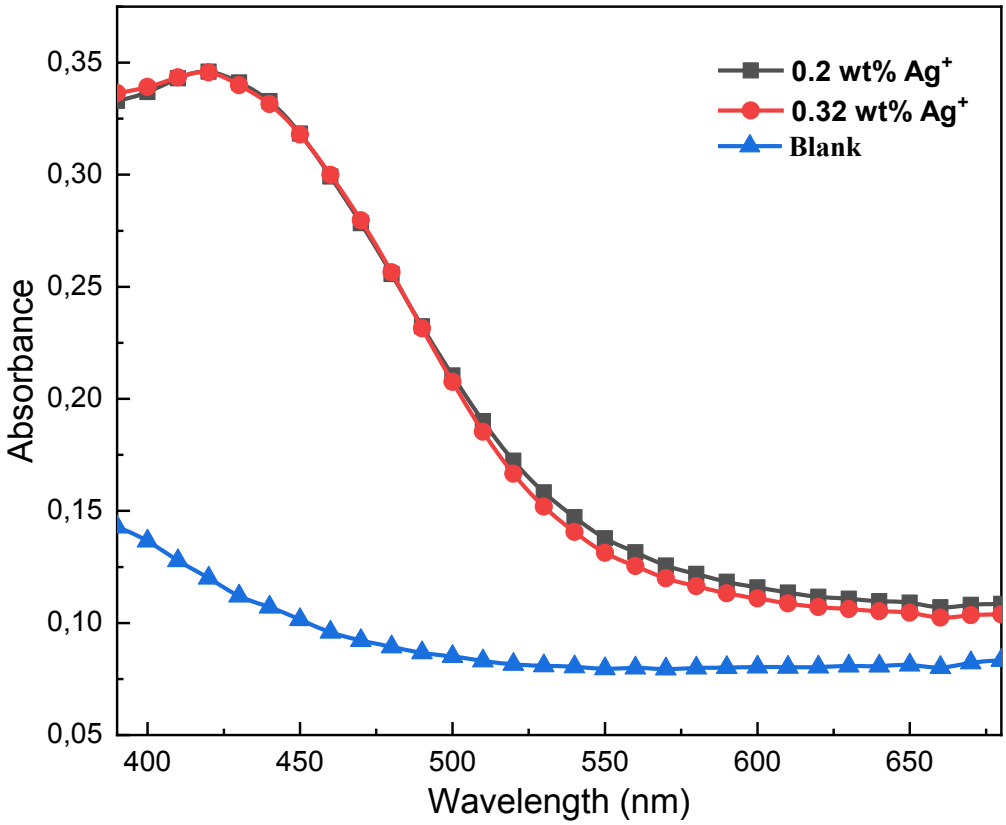

Figure 10. Absorption spectrum of AgNP-Enocell pulp at different concentrations

In order to obtain different colors and to bring more functions into the final Ioncell fibers, silver and gold ions were combined with birch pulp to prepare new composites using the same green reduction method as described above. A series of colors is displayed in Figure 11.

Figure 11. Photography of coated pulp with the combination of AgNPs and AuNPs (Left to right, pure silver ions, with the molar ratios of Ag^{+}/Au^{3+}: 4:1,2:1,1:1,1:2,1:5, the total molar mass is the same for each sample, which is 1.5μmol)

With rising proportion of Au ions, the color became increasingly stronger and changed from yellow to pink. This phenomenon implies that the color caused by AuNPs

takes the predominant role in the mixture of Ag and Au nanoparticles. The reason is that the LSPR effect of AuNPs is stronger than the corresponding impact caused by AgNPs. This hypothesis is also confirmed by the UV reflectance spectrum, in which the PLSR bands resulting from AuNPs were dramatically stronger than the bands from AgNPs. Only for the pure Ag samples, the SPB can be observed, but the signal was quite weak, while for Au samples, each sample containing AuNPs shows a SPB, although these peaks turned into quite flat and weak when the ratio of Ag/Au was higher than 1:1. In comparison, when the ratio of Ag/Au was lower than 1:1, the peak becomes increasingly stronger and sharper, even better than the reference sample of pure 0.06%wt AuNPs. This fact indicates that the addition of Ag ions is able to enhance the effect of PLSR and to control the size distribution of AuNPs to some extent. As to why the SPB of AgNPs becomes weaker in the presence of AuNPs, we assume that there are some inter-coupling reactions between AgNPs and AuNPs, thereby reducing the PLSR effect of AgNPs. In addition, the roughness of the pulp sheets is another factor that affects the reflectance spectrum, as the roughness can cause light scattering that makes the absorption uneven.

In a similar manner, the absorbance spectrum and CIE **L**, **a**, **b** value were shown in Figure 12 and Table 8 to verify the change of color. The higher **L** value and nearly zero of **a** and **b** values indicated that the untreated sample was white. The change of **L**, **a** and **b** values proved the formation of AgNPs and AuNPs, as these nanoparticles would create colors due to the LSPR phenomenon.

Table 8. Reflectance values of AgNPs-AuNPs Enocell pulp of various ratios (Total molar mass of metals on pulp for each recipe is the same, which is 0.15μmol)

Molar Ratios(Ag^{+}/Au^{3+})	4:1	2:1	1:1	1:2	1:5	0:3	Blank
L	74,33	73,32	75,51	87,17	80,18	74,284	92,92
a	15,44	16,12	13,53	-0,14	9,64	11,893	-0,96
b	6,40	4,65	8,13	19,51	10,61	1,558	2,80

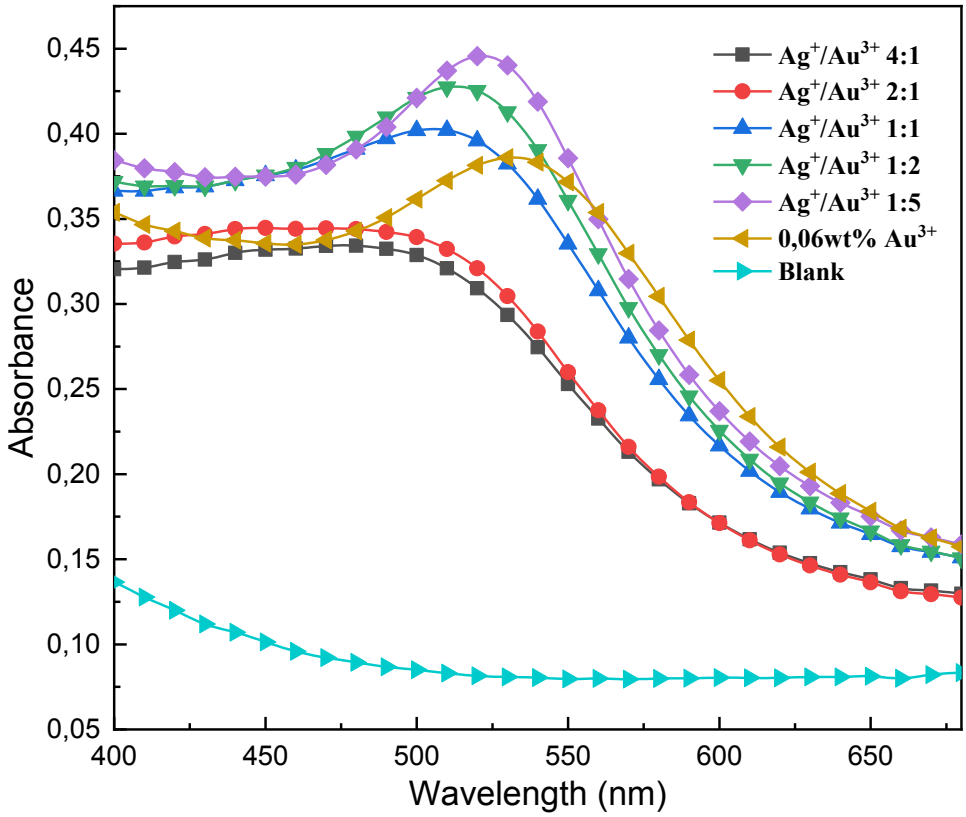

Figure 12. Absorption spectrum of AgNPs-AuNPs Enocell pulp with different molar ratios (Total molar mass of metals on pulp for each recipe is the same, which is 1.5μmol)

4.2.3 Adding order of Au^{3+} and Ag^{+}

It has been reported that adding metal ions separately would enhance the color strength compared to adding both ions in one step.[10] Another group published that the addition order of Ag^{+} and Au^{3+} could affect the formation of nanoparticles, and even generate a core-shell structure.[70] Hence, this section is intended to determine whether AuNPs can react with Ag^{+} and vice versa.

However, we found that the formed Au or Ag NPs did not react with Ag^{+} or Au^{3+}, although there should be certain possibilities according to their redox potential. In general, Ag^{+} could be reduced to Ag in the presence of Au. It might be explained as follows: Both the added Ag^{+} and the formed AuNPs are immobilized onto different reaction sites (hydroxyl groups), preventing them from connecting to each other and hindering the reaction. If these results of the addition of Au^{3+} and Ag^{+} are compared

separately with the result of the simultaneous addition, UV reflectance spectra and CIElab values usually appear to be the same. Consequently, the addition of two types of metals in different orders could not impact on the color and the formation of nanoparticles. (*Here the experimental number is defined according to varying recipes, the specific information had been contained in table 4.*)

Table 9. Reflectance values of coated pulp with different addition order of Ag^{+}/Au^{3+} (No.1/2: Au^{3+} (1μmol/0.5μmol) added first, Ag^{+} (0.5μmol/1μmol) added last; No.3/4: Ag^{+}(0.5µmol /1µmol) added first, Au^{3+} (1µmol /0.5µmol) added last)

Experimental No.	NO.1	NO.3	NO.2	NO.4
L	72,84167	73,33667	76,758	77,32833
a	16,4	17,11833	13,9	11,335
b	3,458333	7,698333	13,02	7,678333

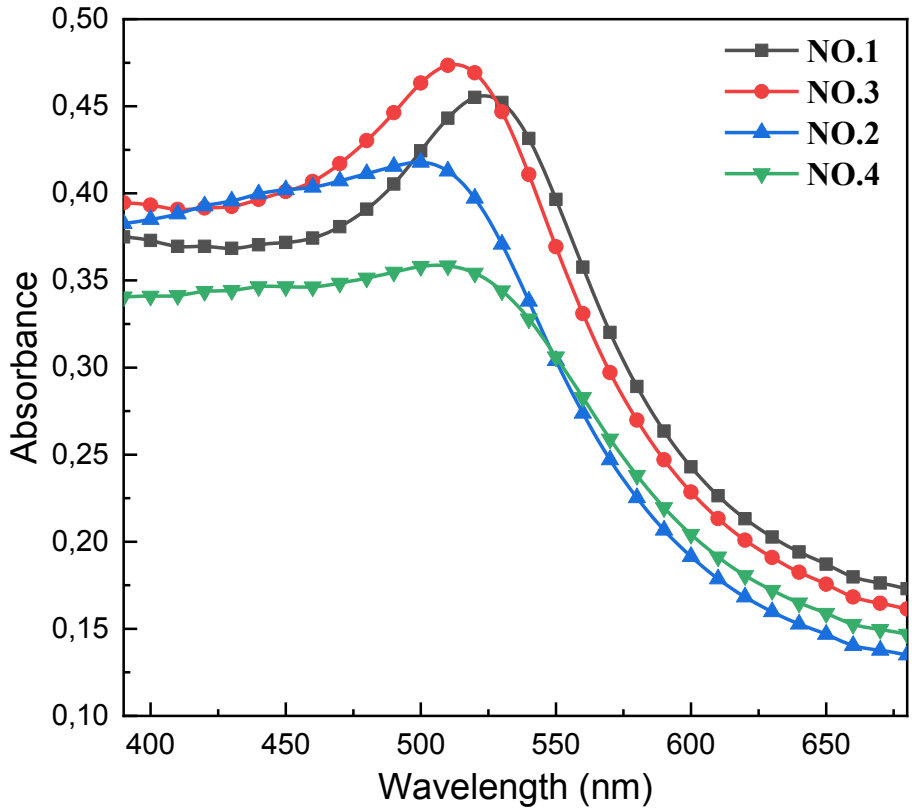

Figure 13. Absorption spectrum of samples with different addition orders of Ag^{+}/Au^{3+}

4.2.4 The addition of CTAB

CTAB as a surfactant is quite critical in the formation of gold nanoparticles due to its controlling function in the growth and shape of gold nanoparticles.[71] Indeed, the

literature to date has shown that CTAB was able to support the formation of rod-shaped micelles and induce an anisotropic growth of gold nanoparticles, thereby controlling the morphology of AuNPs.[72] However, the use of CTAB has been studied only in the seed-mediated method for preparing gold nanoparticles or gold nanorods until now.[73] In this section, we mainly focus on the effect of CTAB in the preparation of gold nanoparticles using the in-situ reduction method based on cellulose.

Figure 12 demonstrates that with increasing the addition of 50mM CTAB, the maximum absorption value reveals a downtrend trend. The plasmon resonance bands show a blue shift, moving towards lower wavelengths. Accordingly, we can assume that the addition of CTAB blocks the formation of AuNPs, but increases their sizes slightly, in comparison with the reference sample. As far as the CIElab value is concerned, the values of the samples have decreased slightly compared to the reference, indicating that the color resulting from AuNPs has become weaker.

It can be assumed that CTAB reacts with $HAuCl_4$ in aqueous solution, forming an organic salt $[CTA]^-[AuBr_4]$, leading to CTAB micelles generating "metallomicelles." The overall reaction scheme is demonstrated below.

$$[\boldsymbol{AuCl_4}]^- + \boldsymbol{4CTAB} \rightarrow \boldsymbol{CTA^-[AuBr_4]^+ + 4Cl^- + 3CTA^+}$$

This organic salt [CTA]-$[AuBr_4]$ is stable and cannot disassociate into gold ions because of its relatively low standard redox potential. In this way, a part of the gold ions is used to form [CTA]-$[AuBr_4]$ and thus is never involved in the reduction reaction for the AuNP synthesis, thereby decreasing the formation of gold nanoparticles.

Table 10. Reflectance values of AuNPs Enocell pulp with the addition of different moles of CTAB (Contents of 0,06wt% Au^{3+})

Addition amount of CTAB (mmol)	**0.5**	**0.35**	**0.25**	**0.1**	**Reference (0.06wt% Au^{3+}, without CTAB)**
L	79,812	75,59	75,616	73,895	74,284
a	3,558	5,758	6,312	8,334	11,893
b	-3,248	-4,578	-3,221	-3,98	1,558

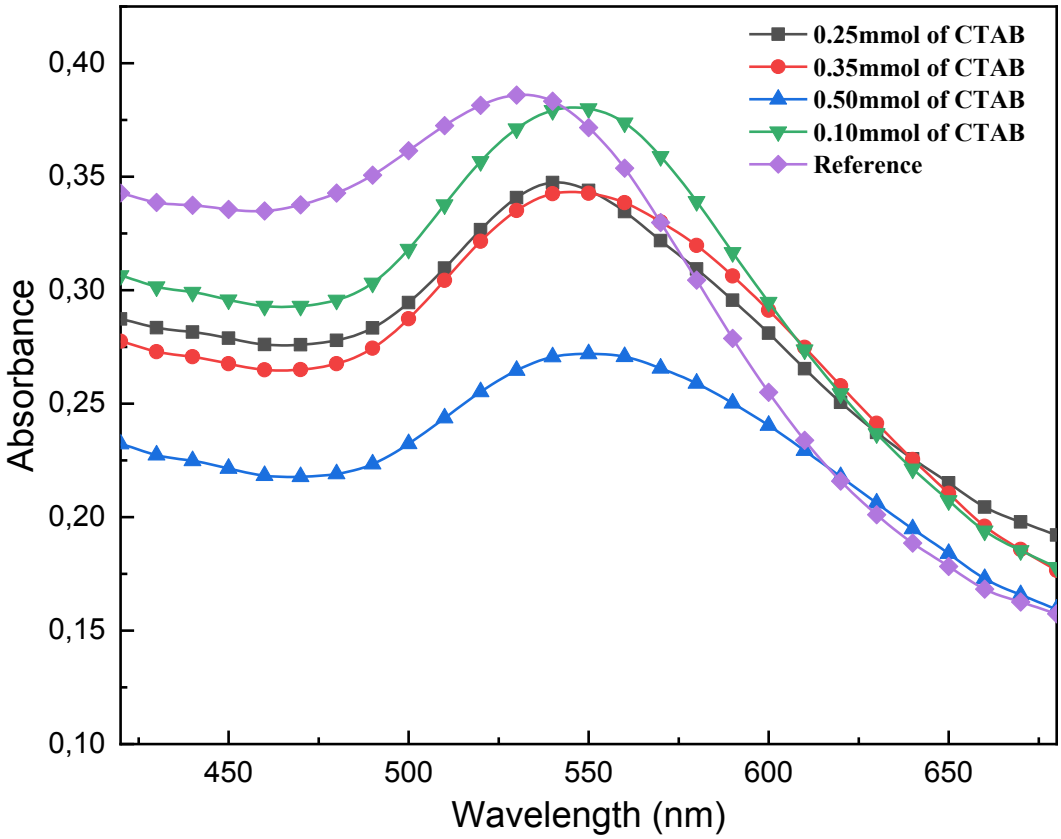

Figure 14. Absorption spectra of AuNPs-Enocell pulp with of various moles of CTAB (Contents of 0.06wt% Au^{3+})

4.2.5 TEM images of AuNPs-Enocell pulp

TEM was performed to verify the formation of gold nanoparticles onto the cellulose pulp.

As shown in images below, the shape of the obtained AuNPs varies, including cubic and round shaped. In addition, we observed that with an increase in wt% of gold ions, the amount of AuNPs formed increased, leading to a high density, while their size decreased gently. On the contrary, lower wt% yielded less AuNPs, which however showed larger sizes.

As far as the size distribution is concerned, although only a few large AuNPs formed, the gold nanoparticles have a similar size on average and do not produce large aggregates.

These facts also correspond to the results of the UV reflectance spectra.

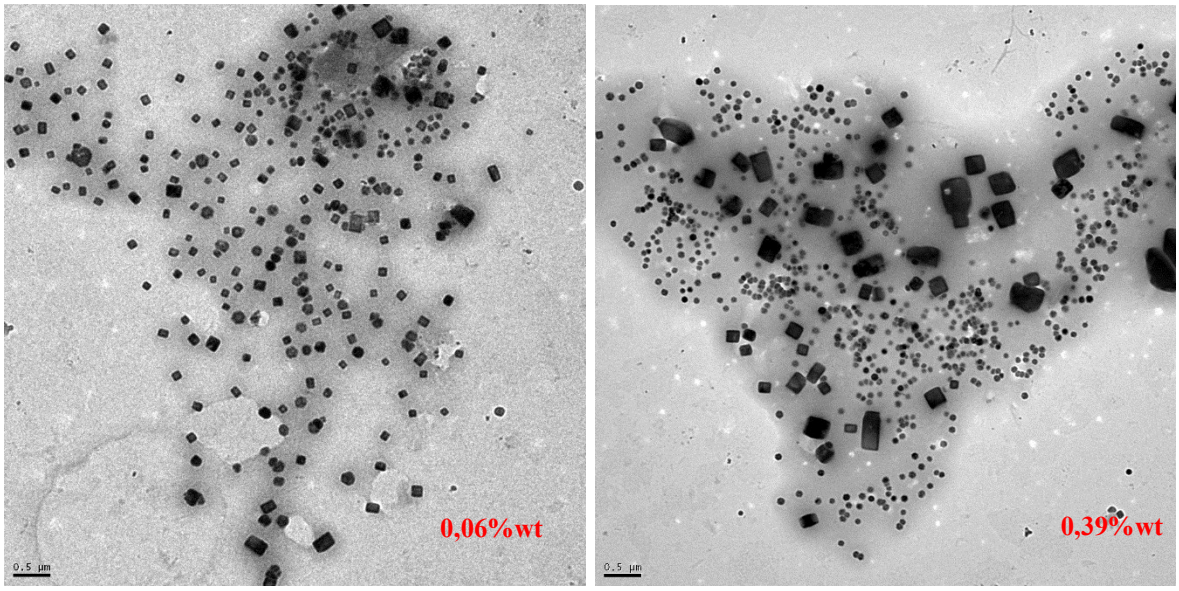

Figure 15. TEM images of AuNPs on the AuNPs-Eocell pulp, Au^{3+} (a)0.06wt% (b) 0.39wt%.

4.3 Characterization of AuNPs-fibers and Au/AgNPs-fibers

4.3.1 Mechanical properties

The strength of a fabric is the most critical factor concerning its final application.

In this study, the Au-Ioncell fibers spun from 13% cellulose concentration were studied for their mechanical properties. Draw ratio (DR), as one of important parameter in the spinning process, should be proportional to the orientation of fibers within the certain range. When DR exceeds the maximum, the intermolecular interactions start to break and thus cause an adverse effect on the polymer structure, compromising the mechanical properties of fibers. In this context, we have chosen 12 as the spinning draw ratio for the production of the Au- Ioncell fibers, as under this condition fibers receive the highest orientation without impairment and at the same time the target fiber thickness (titer). With an increase of DR, the stress behavior of the polymer would be stronger and the cellulose polymer chains would be aligned parallel to the longitudinal axis. The polymer molecules are then firmly compacted, which increases the forces between the cellulose chains.

At the same time the crystallinity increases, which contributes significantly to the

increase in tensile strength and the storage modulus as well as to a lower elongation.[73]

Table 11. Mechanical properties of AuNPs-Ioncell (0.06%wt Au^{3+}); Au/AgNPs-Ioncell(molar ratios of Au^{3+}/Ag^{+}: 1/1), and standard Ioncell(without additives)

	AuNPs-Ioncell	**Au/AgNPs-Ioncell**	**Ioncell**
Linear density (dtex)	1,33±0,08	1,39±0,13	1,42±0,08
Conditioned tenacity (cN/tex)	49,55±2,93	52,77±1,85	47,41±3,3
Conditioned elongation (%)	11,6±1,51	13,2±1,28	12,03±1,8
Wet tenacity (cN/tex)	45,87±1,74	46.62±4,06	44,84±3,14
Wet elongation (%)	6,24±0,44	14.96±1,25	15,19±0,91
Conditioned Fiber diameter (µm)	10,63	10.74	10,98

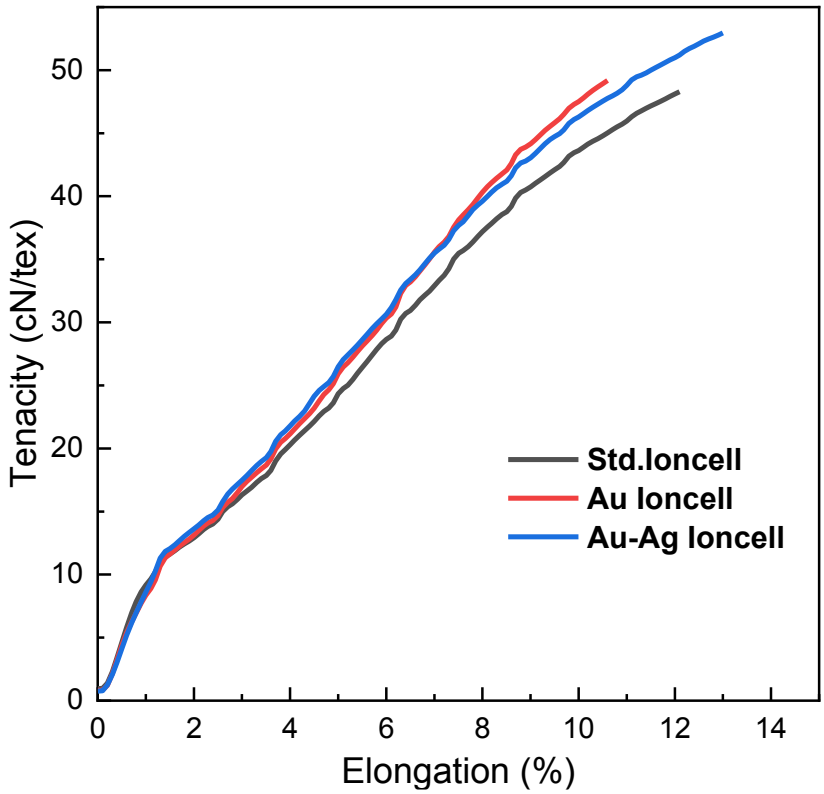

Figure 16. Stress-strain curves of different fibers under conditioned state AuNPs-Ioncell(0.06%wt Au^{3+}); Au/AgNPs-Ioncell(molar ratios of Au^{3+}/Ag^{+}: 1/1, total amount metals 0.06%), standard Ioncell(without additives)

As can be seen, the AuNPs-Ioncell fibers and Au/AgNPs-Ioncell fibers have higher tenacity and lower elongation than the standard Ioncell fibers. It could be explained as follows: Gold nanoparticles tend to fill into ‘gaps’ in the cellulose structure, and the

free volume within cellulose chains is reduced. More polymer molecules are then interconnected by AuNPs, which greatly increases the cross-linking density of cellulose chains. AuNPs with a high inherent modulus also behave as rigid modifier particles, which can contribute to the improvement of strength and modulus. Finally, the presence of nanoparticles between the voids of the molecular chains limit the segmental chain movements, which increases the flexibility and thus the stiffness of fibers.[74]

In a word: gold nanoparticles, which act as a bridge function, make it possible to strengthen the bonding forces between the fiber matrix and improve the mechanical properties of the Au-Ioncell fiber.

Under wet condition, the tensile strength shows a similar trend. However, the strength is gently weaker than in the conditioned state, since the hydrogen bond network in the amorphous regions is partially destroyed after water absorption and swelling. Hence, the proportion of available hydrogen bonds in the amorphous sections could be estimated with the ratio of wet-to-dry tenacity. Swelling should be responsible for the reduction of the bonds in the crystalline region, as it affects the surface area of ordered regions.[73]

4.3.2 Yarn analysis

Yarn spinning is necessary for fibers when it comes to producing knitted patterns. The rigidity of fibers and cohesion of the fiber network are two critical properties for successful yarn spinning. For commercial use, the mechanical property of yarn is the most important indicator, which has been summarized in Table 12. The mechanical properties of yarn depend on a couple of factors: length, fineness, strength, and extension of the fibers. As for yarn count, it is estimated by dividing the linear density of the yarn by the linear density of the separate fibers. The reason to double the linear density of a yarn is to take the resistance force to tension applied in the yarn weaving process into consideration. The coefficient of variation (CV, %) represents the anomaly of spun yarn. The smaller this value is, the more homogeneous the spun yarn. However, it is challenging to calculate the CV of different yarns due to the varying fiber counts.

Hence, the equation below is introduced for a better comparison.

$$I = \frac{CV}{CV_{lim}}$$

$$CV_{lim} = \frac{1}{\sqrt{n}} * 100\%$$

Where CV_{lim} stands for the limit coefficient of variation, and n represents the fiber count.

The higher CV value can be explained by the higher fiber fineness originating from this experiment. And the other reason is the deviation of the fiber length since the cutting of the filaments was carried out by hand and not on a standardized machine.[66]

Table 12. Mechanical properties of AuNPs-Ioncell yarn (1.5μmol,0.06%wt Au^{3+}) and Standard-Ioncell yarn(Without the contents of Au^{3+})

Parameters	Tex (g/1000m)	Tex	Elongation (%)	Breaking force(cN)	Tenacity(cN/tex)
AuNPs-Ioncell yarn	22,11	22,15	6,41	445,79	20,43
CV%	13,6	23,21	16,6	28,6	24,8
Standard-Ioncell yarn	22,9	22,0	7,19	586,79	26,67
CV%	4,86	7,3	9,24	10,98	8,36

4.3.3 The distribution of AuNPs on the AuNPs-Ioncell fibers

In order to detect the distribution of AuNPs on the AuNPs-Ioncell fibers, SEM (Phenom Prox) with back scattered mode was employed. These light spots should be AuNPs, as relatively heavier atoms display bright colors compared to atoms with smaller relative atomic mass under the back scattered mode of SEM. According to the SEM images, the AuNPs are homogeneously distributed on the fiber surface.

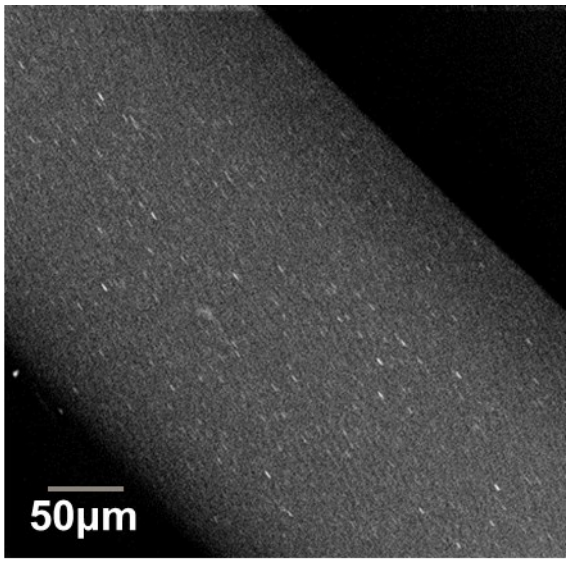

Figure 17. AuNPs distribution on the surface of Ioncell-fibers (0,06wt% Au^{3+})

4.3.4 The molecular mass distribution of cellulose

In order to verify whether the coating process affects the degree of polymerization, the molecular mass distribution of pulp before coating and after coating was measured by gel permeation chromatography (GPC). Figure 14 illustrates that Enocell pulp treated with Au degrades only slightly. The results show that the in-situ reduction method hardly affects the molecular chain length of cellulose, and the macromolecular properties of the fibers spun from AuNPs-Enocell did not deviate from fibers produced from virgin material.

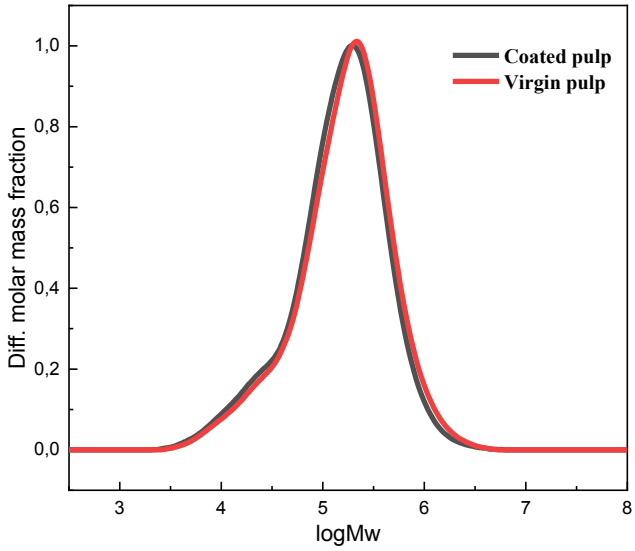

Figure 18. The molar mass distribution of coated and virgin pulp

4.3.5 The comparison of AuNPs and Au/AgNPs Enocell pulp and the corresponding spun fibers

The absorption spectra were measured to study the effect of the spinning process on the AuNPs.

From these spectra, the absorption bands become higher and wider after spinning than before spinning, indicating that the AuNPs size distribution became broader during spinning.

With regard to the increased f absorption peak, there are two explanations. One is that spinning conditions such as high temperature and high pressure continue the reduction reaction of AuNPs and form more AuNPs. The other is that the presence of the ionic liquid and the mechanical process itself reshape the AuNPs to yield other shapes which possess a stronger plasmon resonance effect.

Table 13. Reflectance values of samples of AuNPs-pulp (1.5μmol; 0.06%wt Au^{3+}); Au/AgNPs-pulp (molar ratio of Au^{3+}/Ag^{+}: 1/1, total amount of metals is 1.5μmol), and corresponding spun fibers

	Before spinning(AuNPs)	**After spinning(AuNPs)**	**Before spinning(Au/AgNPs)**	**After spinning(Au/AgNPs)**
L	74,28	65,438	75,51	66,821
a	11,89	3,887	13,53	5,207
b	1,558	-0,153	8,13	4,292

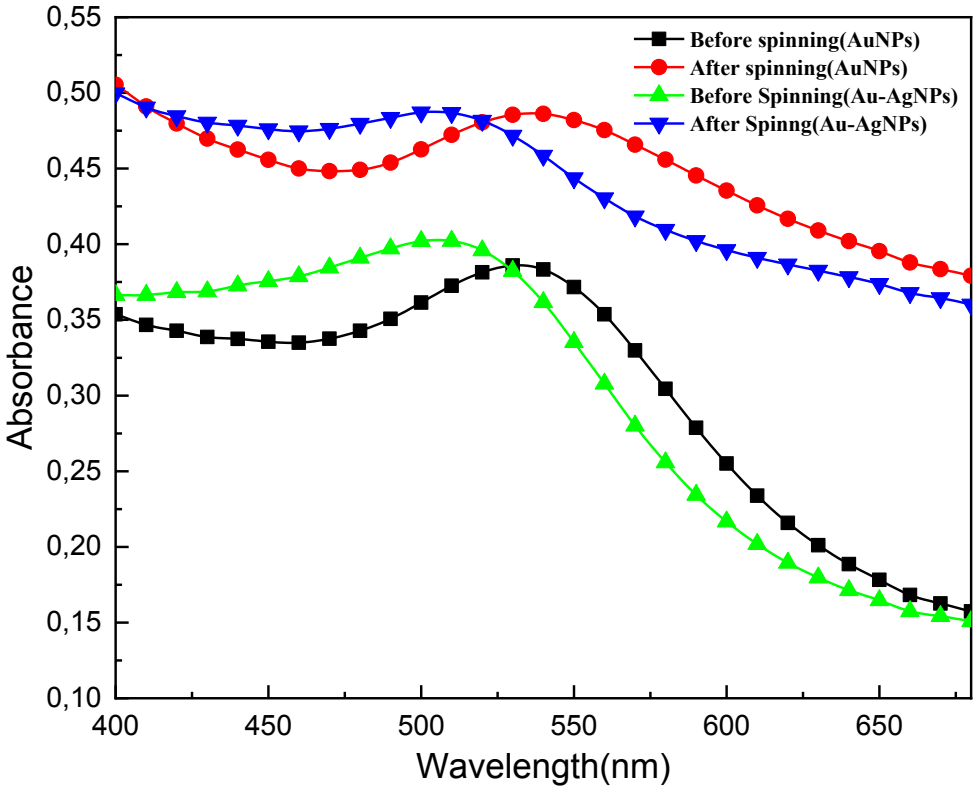

Figure 19. Absorption spectrum from AuNPs-pulp (0.06%wt Au^{3+}); Au/AgNPs-pulp (molar ratios of Au^{3+}/Ag^{+}: 1/1, total amount of metals: 1.5μmol) and corresponding spun fibers

4.3.6 Washing fastness

Poor colorfastness in textile products is a major source of customer complaints. The color fastness can vary depending on the type of dye, the shades used, the color depth and the execution of the dyeing process. Hence, the color fastness properties of fibers must be taken into account if they are to be used in industrial production.

Here, the fibers before and after washing with a detergent were measured. Along with the basis of the gray scale, the difference of colors was quantified as in the equations below. **E** represents the total color difference of the fabric before and after washing. In these formulas, **L** is the lightness dimension, **a** and **b** are the color-opponent dimensions. The subscripts 0 and 1 represent the samples before and after washing, respectively.

$$E = \sqrt{\Delta L^2 \ + \ \Delta a^2 \ + \ \Delta b^2}$$

Where $\Delta L = L_0 - L_1;\ \ \Delta a = a_0 - a_1;\ \ \Delta b = b_0 - b_1$

Table 14 summarizes the result before and after testing. The very small E value implies that the color difference is quite small. This result proves that Ioncell fabrics treated with AuNPs have excellent colorfastness properties against washing in contrast the direct coating method as reported. [11] In addition, as reported by the master thesis from our group,[75] the color difference of textiles dyed by vat and reactive dyes varied ranging 4-32 according to various dyes. This indicated that the stability of color from AuNPs are stronger than the conventional dyes.

Table 14. Reflectance values of before and after washing with detergent (AuNPs-Ioncell fibers, 0.06wt% Au^{3+})

	Before washing	**After washing**
L	57,6	56,81
a	5,284	4,646
b	0,319	0,487
E	1,032	

5. Conclusion

AuNPs are widely utilized in the apparel sector because they not only dye fabrics as pigments do but also functionalize fabrics to show more properties such as UV-protection and anti-bacterial behavior. In this master thesis, AuNPs were prepared by reduction of chloroauric acid (CA) in situ on bleached birch pulp to form cellulose-AuNPs hybrids. The pulp was colored by the AuNPs due to their localized surface plasmon resonance (LSPR) properties. After dissolving in [DBNH] OAc, these colored pulps were processed into fibers by dry-jet wet spinning.

During this process, factors such as the amount of CA solution added, the pH, the addition of CTAB, and the combination with silver ions were studied. Among the relatively low wt% (weight percentage) of CA, the yield of AuNPs increased but showed decreasing sizes. As soon as the wt% were above the threshold, the color of the

pulp began to fade until it became colorless. With regard to the pH, the results showed that either acidic or alkaline conditions negatively affect the yield of AuNPs, while accelerating the reaction rate. This method can also be applied to silver ions.

We were able to produce AgNPs on bleached pulp, which displayed a yellow color due to a different LSPR. CTAB, as a frequently used surfactant, was studied additionally in this thesis. The results demonstrated that the addition of CTAB would inhibit the contact between gold ions and the cellulose dispersion, thereby preventing the formation of AuNPs.

The fabrics prepared by cellulose-AuNPs showed excellent stability of the AuNPs to the pulp after the color fastness tests. Furthermore, the addition of AuNPs or/and AgNPs can improve the mechanical properties of spun fibers.

Due to the time limit, further experiments will have to be carried out in future work. In order to test the anti-bacterial properties of the obtained fabrics, to investigate the distribution of AuNPs and AgNPs in the filaments and to prepare the fabrics coated with pure AgNPs denote some experiments which need to be accomplished in the future.

6. Reference

1. Amin M, Iram F, Iqbal MS, Saeed MZ, Raza M, Alam S. Arabinoxylan-mediated synthesis of gold and silver nanoparticles having exceptional high stability. *Carbohydr Polym*. 2013;92(2):1896-1900. doi:10.1016/j.carbpol.2012.11.056
2. Aromal SA, Philip D. Benincasa hispida seed mediated green synthesis of gold nanoparticles and its optical nonlinearity. *Phys E Low-dimensional Syst Nanostructures*. 2012;44(7-8):1329-1334. doi:10.1016/J.PHYSE.2012.02.013
3. Azetsu A, Koga H, Isogai A, Kitaoka T. Synthesis and Catalytic Features of Hybrid Metal Nanoparticles Supported on Cellulose Nanofibers. *Catalysts*. 2011;1(1):83-96. doi:10.3390/catal1010083
4. Rodríguez-Lorenzo L, Álvarez-Puebla RA, de Abajo FJG, Liz-Marzán LM. Surface Enhanced Raman Scattering Using Star-Shaped Gold Colloidal Nanoparticles. *J Phys Chem C*. 2010;114(16):7336-7340. doi:10.1021/jp909253w
5. Ming T, Chen H, Jiang R, Li Q, Wang J. Plasmon-Controlled Fluorescence: Beyond the Intensity Enhancement. *J Phys Chem Lett*. 2012;3(2):191-202. doi:10.1021/jz201392k
6. Huang X, Neretina S, El-Sayed MA. Gold nanorods: From synthesis and properties to biological and biomedical applications. *Adv Mater*. 2009;21(48):4880-4910. doi:10.1002/adma.200802789
7. Bobin O, Schvoerer M, Ney C, et al. The role of copper and silver in the colouration of metallic luster decorations (Tunisia, 9th century; Mesopotamia, 10th century; Sicily, 16th century): A first approach. *Color Res Appl*. 2003;28(5):352-359. doi:10.1002/col.10183
8. Johnston JH, Nilsson T. Nanogold and nanosilver composites with lignin-containing cellulose fibres. *J Mater Sci*. 2012;47(3):1103-1112. doi:10.1007/s10853-011-5882-0
9. Tang B, Yao Y, Li J, et al. Functional Application of Noble Metal Nanoparticles In Situ Synthesized on Ramie Fibers. *Nanoscale Res Lett*. 2015;10(1):1-9. doi:10.1186/s11671-015-1074-1
10. Tang B, Sun L, Kaur J, Yu Y, Wang X. In-situ synthesis of gold nanoparticles for multifunctionalization of silk fabrics. *Dye Pigment*. 2014;103:183-190. doi:10.1016/j.dyepig.2013.12.008
11. Zheng Y, Xiao M, Jiang S, Ding F, Wang J. Coating fabrics with gold nanorods for colouring, UV-protection, and antibacterial functions. *Nanoscale*. 2013;5(2):788-795. doi:10.1039/C2NR33064D
12. Kobayashi S, Kashiwa K, Shimada J, Kawasaki T, Shoda S. Enzymatic polymerization: The first in vitro synthesis of cellulose via nonbiosynthetic path catalyzed by cellulase. *Makromol Chemie Macromol Symp*. 1992;54-55(1):509-518. doi:10.1002/masy.19920540138
13. Klemm D, Heublein B, Fink H-P, Bohn A. Cellulose: Fascinating Biopolymer and Sustainable Raw Material. *Angew Chemie Int Ed*. 2005;44(22):3358-3393. doi:10.1002/anie.200460587
14. Suhas, Gupta VK, Carrott PJM, Singh R, Chaudhary M, Kushwaha S. Cellulose: A review as natural, modified and activated carbon adsorbent. *Bioresour Technol*. 2016;216:1066-1076. doi:10.1016/j.biortech.2016.05.106
15. Morton WE (William E, Hearle JWS, Textile Institute (Manchester E. *Physical Properties of*

Textile Fibres. CRC Press; 2008.

16. Gardner KH, Blackwell J. The structure of native cellulose. *Biopolymers*. 1974;13(10):1975-2001. doi:10.1002/bip.1974.360131005
17. Hinterstoisser B, Salmén L. Application of dynamic 2D FTIR to cellulose. *Vib Spectrosc*. 2000;22(1-2):111-118. doi:10.1016/S0924-2031(99)00063-6
18. Marchessault RH. Cellulose structure modification and hydrolysis, Raymond A. Young and Roger M. Rowell, Eds., Wiley-Interscience, New York, 1986, 379 pp. *J Polym Sci Part C Polym Lett*. 1987;25(3):139-140. doi:10.1002/pol.1987.140250313
19. Brown Jr RM, Saxena IM. Cellulose biosynthesis: A model for understanding the assembly of biopolymers. *Plant Physiol Biochem*. 2000;38(1-2):57-67. doi:10.1016/S0981-9428(00)00168-6
20. Sakurada I, Nukushina Y, Ito T. Experimental determination of the elastic modulus of crystalline regions in oriented polymers. *J Polym Sci*. 1962;57(165):651-660. doi:10.1002/pol.1962.1205716551
21. Nishino T, Takano K, Nakamae K. Elastic modulus of the crystalline regions of cellulose polymorphs. *J Polym Sci Part B Polym Phys*. 1995;33(11):1647-1651. doi:10.1002/polb.1995.090331110
22. Nishino T, Matsuda I, Hirao K. All-Cellulose Composite. *Macromolecules*. 2004;37(20):7683-7687. doi:10.1021/ma049300h
23. Lindman B, Karlström G, Stigsson L. On the mechanism of dissolution of cellulose. *J Mol Liq*. 2010;156(1):76-81. doi:10.1016/J.MOLLIQ.2010.04.016
24. Woodings C, Textile Institute (Manchester E. *Regenerated Cellulose Fibres*. CRC Press; 2001.
25. Rosenau T, Potthast A, Sixta H, Kosma P. The chemistry of side reactions and byproduct formation in the system NMMO/cellulose (Lyocell process). *Prog Polym Sci*. 2001;26(9):1763-1837. doi:10.1016/S0079-6700(01)00023-5
26. Sixta. Ioncell-F: A High-strength regenerated cellulose fibre. *Nord Pulp Pap Res J*. 2015;30(01):043-057. doi:10.3183/NPPRJ-2015-30-01-p043-057
27. Richard P. Swatloski, Scott K. Spear, John D. Holbrey and, Rogers* RD. Dissolution of Cellose with Ionic Liquids. 2002. doi:10.1021/JA025790M
28. Ghandi K. A Review of Ionic Liquids, Their Limits and Applications. *Green Sustain Chem*. 2014;04(01):44-53. doi:10.4236/gsc.2014.41008
29. Rosenau T, Hofinger A, Potthast A, Kosma P. On the conformation of the cellulose solvent N-methylmorpholine-N-oxide (NMMO) in solution. *Polymer (Guildf)*. 2003;44(20):6153-6158. doi:10.1016/S0032-3861(03)00663-3
30. Asaadi S, Hummel M, Hellsten S, et al. Renewable High-Performance Fibers from the Chemical Recycling of Cotton Waste Utilizing an Ionic Liquid. *ChemSusChem*. 2016;9(22):3250-3258. doi:10.1002/cssc.201600680
31. Li R, Chang C, Zhou J, et al. Primarily Industrialized Trial of Novel Fibers Spun from Cellulose Dope in NaOH/Urea Aqueous Solution. *Ind Eng Chem Res*. 2010;49(22):11380-11384. doi:10.1021/ie101144h
32. Liu X, Atwater M, Wang J, Huo Q. Extinction coefficient of gold nanoparticles with different sizes and different capping ligands. *Colloids Surfaces B Biointerfaces*. 2007;58(1):3-7. doi:10.1016/j.colsurfb.2006.08.005
33. Yeh Y-C, Creran B, Rotello VM. Gold nanoparticles: preparation, properties, and applications

in bionanotechnology. *Nanoscale*. 2012;4(6):1871-1880. doi:10.1039/c1nr11188d

34. Sau TK, Rogach AL, Jäckel F, Klar TA, Feldmann J. Properties and Applications of Colloidal Nonspherical Noble Metal Nanoparticles. *Adv Mater*. 2010;22(16):1805-1825. doi:10.1002/adma.200902557
35. Cao J, Sun T, Grattan KTV. Gold nanorod-based localized surface plasmon resonance biosensors: A review. *Sensors Actuators, B Chem*. 2014;195:332-351. doi:10.1016/j.snb.2014.01.056
36. Willets KA, Van Duyne RP. Localized Surface Plasmon Resonance Spectroscopy and Sensing. *Annu Rev Phys Chem*. 2007;58(1):267-297. doi:10.1146/annurev.physchem.58.032806.104607
37. Anker JN, Hall WP, Lyandres O, Shah NC, Zhao J, Van Duyne RP. Biosensing with plasmonic nanosensors. *Nat Mater*. 2008;7(6):442-453. doi:10.1038/nmat2162
38. Eustis S, El-Sayed MA. Why gold nanoparticles are more precious than pretty gold: Noble metal surface plasmon resonance and its enhancement of the radiative and nonradiative properties of nanocrystals of different shapes. *Chem Soc Rev*. 2006;35(3):209-217. doi:10.1039/B514191E
39. Pérez-Juste J, Pastoriza-Santos I, Liz-Marzán LM, Mulvaney P. Gold nanorods: Synthesis, characterization and applications. *Coord Chem Rev*. 2005;249(17-18):1870-1901. doi:10.1016/J.CCR.2005.01.030
40. Jain PK, Lee KS, El-Sayed IH, El-Sayed MA. Calculated Absorption and Scattering Properties of Gold Nanoparticles of Different Size, Shape, and Composition: Applications in Biological Imaging and Biomedicine. *J Phys Chem B*. 2006;110(14):7238-7248. doi:10.1021/jp057170o
41. Allen C. Templeton †, Jeremy J. Pietron †, Royce W. Murray *,† and, Paul Mulvaney* ‡. Solvent Refractive Index and Core Charge Influences on the Surface Plasmon Absorbance of Alkanethiolate Monolayer-Protected Gold Clusters. 1999. doi:10.1021/JP991889C
42. Sharma V, Park K, Srinivasarao M. Colloidal dispersion of gold nanorods: Historical background, optical properties, seed-mediated synthesis, shape separation and self-assembly. *Mater Sci Eng R Reports*. 2009;65(1-3):1-38. doi:10.1016/J.MSER.2009.02.002
43. Hutter E, Fendler JH. Exploitation of Localized Surface Plasmon Resonance. *Adv Mater*. 2004;16(19):1685-1706. doi:10.1002/adma.200400271
44. K.-H. Su, Q.-H. Wei and, Zhang* X, J. J. Mock, D. R. Smith and, Schultz S. Interparticle Coupling Effects on Plasmon Resonances of Nanogold Particles. 2003. doi:10.1021/NL034197F
45. Petryayeva E, Krull UJ. Localized surface plasmon resonance: Nanostructures, bioassays and biosensing—A review. *Anal Chim Acta*. 2011;706(1):8-24. doi:10.1016/J.ACA.2011.08.020
46. Mayer KM, Hafner JH. Localized Surface Plasmon Resonance Sensors. *Chem Rev*. 2011;111(6):3828-3857. doi:10.1021/cr100313v
47. Peter N. Njoki, I-Im S. Lim, Derrick Mott, et al. Size Correlation of Optical and Spectroscopic Properties for Gold Nanoparticles. 2007. doi:10.1021/JP074902Z
48. Hu M, Chen J, Li Z-Y, et al. Gold nanostructures: engineering their plasmonic properties for biomedical applications. *Chem Soc Rev*. 2006;35(11):1084. doi:10.1039/b517615h
49. Pérez-Juste J, Pastoriza-Santos I, Liz-Marzán LM, Mulvaney P. Gold nanorods: Synthesis, characterization and applications. *Coord Chem Rev*. 2005;249(17-18):1870-1901. doi:10.1016/J.CCR.2005.01.030
50. S. Link, M. B. Mohamed and, El-Sayed* MA. Simulation of the Optical Absorption Spectra

of Gold Nanorods as a Function of Their Aspect Ratio and the Effect of the Medium Dielectric Constant. 1999. doi:10.1021/JP990183F

51. Zhang T, Wang W, Zhang D, et al. Biotemplated Synthesis of Gold Nanoparticle–Bacteria Cellulose Nanofiber Nanocomposites and Their Application in Biosensing. doi:10.1002/adfm.200902104
52. Grzelczak M, Vermant J, Furst EM, Liz-Marzán LM. Directed Self-Assembly of Nanoparticles. *ACS Nano*. 2010;4(7):3591-3605. doi:10.1021/nn100869j
53. B. Pinto RJ, C. M, Pascoal C, Trindade T. Composites of Cellulose and Metal Nanoparticles. In: *Nanocomposites - New Trends and Developments*. InTech; 2012. doi:10.5772/50553
54. Lam E, Hrapovic S, Majid E, Chong JH, Luong JHT. Catalysis using gold nanoparticles decorated on nanocrystalline cellulose. *Nanoscale*. 2012;4(3):997. doi:10.1039/c2nr11558a
55. Wu D, Fang Y. The adsorption behavior of p-hydroxybenzoic acid on a silver-coated filter paper by surface enhanced Raman scattering. *J Colloid Interface Sci*. 2003;265(2):234-238. http://www.ncbi.nlm.nih.gov/pubmed/12962655. Accessed April 25, 2018.
56. Ma W, Fang Y. Experimental (SERS) and theoretical (DFT) studies on the adsorption of p-, m-, and o-nitroaniline on gold nanoparticles. *J Colloid Interface Sci*. 2006;303(1):1-8. doi:10.1016/J.JCIS.2006.05.001
57. Dong BH, Hinestroza JP. Metal Nanoparticles on Natural Cellulose Fibers: Electrostatic Assembly and In Situ Synthesis. *ACS Appl Mater Interfaces*. 2009;1(4):797-803. doi:10.1021/am800225j
58. Sahoo GP, Bhui DK, Bar H, et al. Synthesis and characterization of gold nanoparticles adsorbed in methyl cellulose micro fibrils. *J Mol Liq*. 2010;155(2-3):91-95. doi:10.1016/J.MOLLIQ.2010.05.013
59. Boufi S, Ferraria AM, do Rego AMB, Battaglini N, Herbst F, Vilar MR. Surface functionalisation of cellulose with noble metals nanoparticles through a selective nucleation. *Carbohydr Polym*. 2011;86(4):1586-1594. doi:10.1016/J.CARBPOL.2011.06.067
60. Koga H, Tokunaga E, Hidaka M, et al. Topochemical synthesis and catalysis of metal nanoparticles exposed on crystalline cellulose nanofibers. *Chem Commun*. 2010;46(45):8567. doi:10.1039/c0cc02754e
61. Yokota S, Kitaoka T, Sugiyama J, Wariishi H. Cellulose I Nanolayers Designed by Self-Assembly of its Thiosemicarbazone on a Gold Substrate. *Adv Mater*. 2007;19(20):3368-3370. doi:10.1002/adma.200602761
62. Junhui He †, Toyoki Kunitake *,† and, Nakao‡ A. Facile In Situ Synthesis of Noble Metal Nanoparticles in Porous Cellulose Fibers. 2003. doi:10.1021/CM034720R
63. Ngo YH, Li D, Simon GP, Garnier G. Gold Nanoparticle–Paper as a Three-Dimensional Surface Enhanced Raman Scattering Substrate. *Langmuir*. 2012;28(23):8782-8790. doi:10.1021/la3012734
64. Zhang L, Li X, Ong L, et al. Cellulose nanofibre textured SERS substrate. *Colloids Surfaces A Physicochem Eng Asp*. 2015;468:309-314. doi:10.1016/j.colsurfa.2014.12.056
65. Mohamed MM, Fouad SA, Elshoky HA, Mohammed GM, Salaheldin TA. Antibacterial effect of gold nanoparticles against Corynebacterium pseudotuberculosis. *Int J Vet Sci Med*. 2017;5(1):23-29. doi:10.1016/J.IJVSM.2017.02.003
66. Michud A, Tanttu M, Asaadi S, et al. Ioncell-F: ionic liquid-based cellulosic textile fibers as an alternative to viscose and Lyocell. *Text Res J*. 2016;86(5):543-552.

doi:10.1177/0040517515591774

67. Wise L. Chlorite holocellulose, its fractionation and bearing on summative wood analysis and studies on the hemicelluloses. *Pap Trade J*. 1946. http://www.worldcat.org/title/chlorite-holocellulose-its-fractionation-and-bearing-on-summative-wood-analysis-and-studies-on-the-hemicelluloses/oclc/708721051. Accessed June 18, 2018.
68. Junhui He †, Toyoki Kunitake *,† and, Nakao‡ A. Facile In Situ Synthesis of Noble Metal Nanoparticles in Porous Cellulose Fibers. 2003. doi:10.1021/CM034720R
69. Pavasars I, Hagberg J, Borén H, Allard B. Alkaline Degradation of Cellulose: Mechanisms and Kinetics. *J Polym Environ*. 2003;11(2):39-47. doi:10.1023/A:1024267704794
70. Tsai TT, Huang TH, Chang CJ, Yi-Ju Ho N, Tseng YT, Chen CF. Antibacterial cellulose paper made with silver-coated gold nanoparticles. *Sci Rep*. 2017;7(1):1-10. doi:10.1038/s41598-017-03357-w
71. and DKS, Korgel* BA. The Importance of the CTAB Surfactant on the Colloidal Seed-Mediated Synthesis of Gold Nanorods. 2008. doi:10.1021/LA703625A
72. Smith DK, Korgel BA. The importance of the CTAB surfactant on the colloidal seed-mediated synthesis of gold nanorods. *Langmuir*. 2008;24(3):644-649. doi:10.1021/la703625a
73. P re p a ra tio n a n d Gro w th Me c h a n is m o f Go ld N a n o ro d s (N Rs) U s in g S e e d -Me d ia te d Gro w th Me th o d. 2003;(16):1957-1962.
74. Zheng Y, Ning R, Zheng Y. Study of SiO2 nanoparticles on the improved performance of epoxy and fiber composites. *J Reinf Plast Compos*. 2005;24(3):223-233. doi:10.1177/0731684405043552
75. Smirnova E. Masters thesis 2017 aalto university school of arts design and architecture fashion and collection design eugenia smirnova. 2017.

Appendix

1. Photography of yarn and textiles made from AuNPs Ioncell fibers

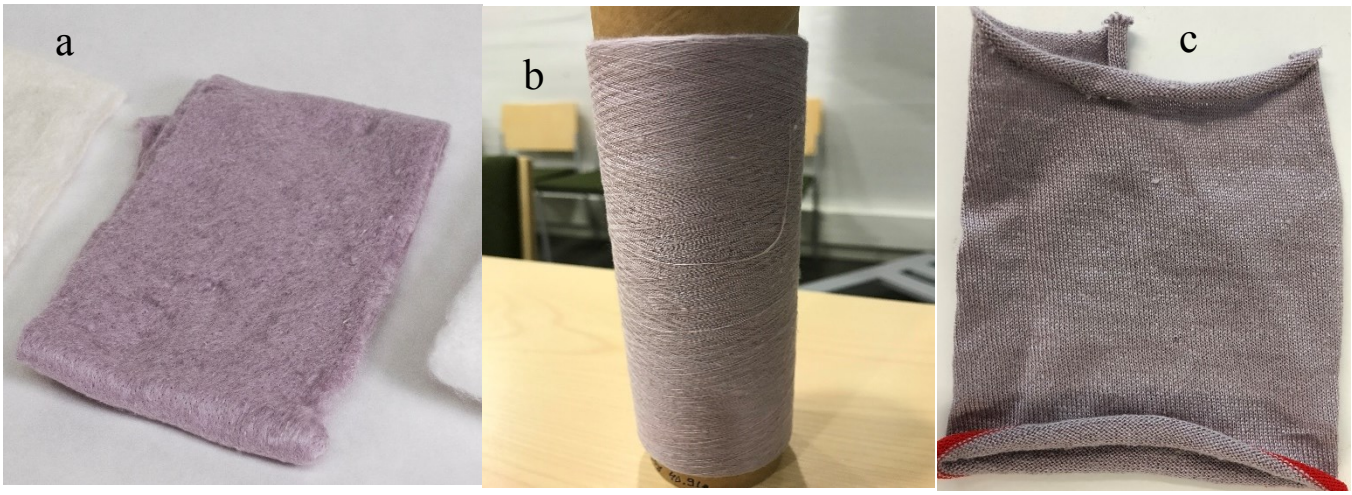

Figure A1 Photography of (a) non-wounven sample (b)yarn (c)knitted sample.
Produced by AuNPs-pulp, 0.06wt%

Figure A2. Photography of (a) non-wounven sample (b)yarn (c)knitted sample.
Produced by AuNps/AgNPs-pulp, ratio of 1/1

3. The calculation process of wt% of gold ions to pulp

The calculation process of the first recipe in table1 at experimental section is explained here. In this case, 1.5mL of 50mM $HAuCl_4.3H_20$ solution was added into 0.5g O.D. pulp, so the molarity of $HAuCl_4.3H_20$ should be $7.5*10^{-5}$ mol. Since the atomic weight of Au and $HAuCl_4.3H_2O$ is 196.93g and 393.83g respectively, the mass ratio of Au^{3+} in $HAuCl_4.3H_2O$ was 0.5, which means the molarity of Au^{3+} is $3.75*10^{-5}$ mol, which

amounts to 0.0147g. Hence, the weight ratio of Au^{3+} and Enocell pulp should be 2.95%.

4. Reaction process monitoring pictures under the study of pH

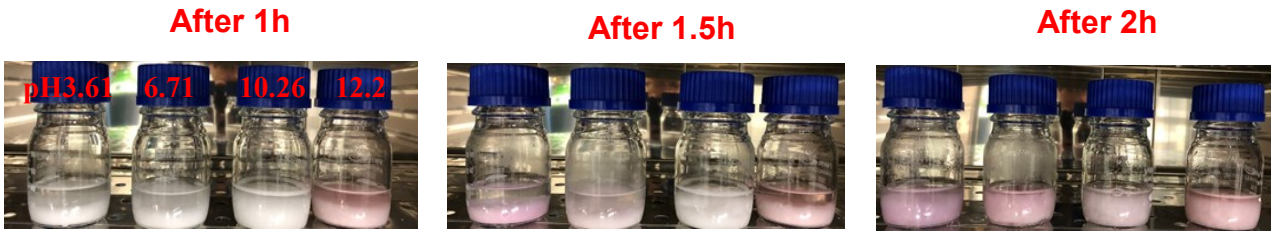

Figure A3. Photography of reaction process regarding the study of factor pH

5. Explanation of remaining work

Due to the limitation of time and technical issues, some complementary experiments should be completed in the near future to ensure the integrity of this thesis topic. All of these experiments had been summarized in the table below.

TableA1. The summary of experiments to be accomplished

	Anti-bacterial testing	UV-protection	GPC	TEM imaging of cross section of fibers
AuNPs-Ioncell	√	√		√
Au/AgNPs-Ioncell	√	√	√	√